

Exposure to an enriched CO₂ atmosphere alters carbon assimilation and allocation in a pine forest ecosystem

KARINA V. R. SCHÄFER*, RAM OREN*, DAVID S. ELLSWORTH†, CHUN-TA LAI‡, JEFFREY D. HERRICK§, ADRIEN C. FINZI¶, DANIEL D. RICHTER*, and GABRIEL G. KATUL*

*Nicholas School of the Environment and Earth Sciences, Box 90328, Durham, NC 27708, USA, †School of Natural Resources and Environment, University of Michigan, 430 E. University Ave., Ann Arbor, MI 48109, USA, ‡Department of Biology, University of Utah, Salt Lake City, UT 84112, USA, §West Virginia University, Morgantown, WV 26506, USA, ¶Department of Biology, Boston University, 5 Cunningham St., Boston, MA 02215, USA

Abstract

We linked a leaf-level CO₂ assimilation model with a model that accounts for light attenuation in the canopy and measurements of sap-flux-based canopy conductance into a new canopy conductance-constrained carbon assimilation (4C-A) model. We estimated canopy CO₂ uptake (A_{nC}) at the Duke Forest free-air CO₂ enrichment (FACE) study. Rates of A_{nC} estimated from the 4C-A model agreed well with leaf gas exchange measurements (A_{net}) in both CO₂ treatments. Under ambient conditions, monthly sums of net CO₂ uptake by the canopy (A_{nC}) were 13% higher than estimates based on eddy-covariance and chamber measurements. Annual estimates of A_{nC} were only 3% higher than carbon (C) accumulations and losses estimated from ground-based measurements for the entire stand. The C budget for the *Pinus taeda* component was well constrained (within 1% of ground-based measurements). Although the closure of the C budget for the broadleaf species was poorer (within 20%), these species are a minor component of the forest. Under elevated CO₂, the C used annually for growth, turnover, and respiration balanced only 80% of the A_{nC} . Of the extra 700 g C m⁻² a⁻¹ (1999 and 2000 average), 86% is attributable to surface soil CO₂ efflux. This suggests that the production and turnover of fine roots was underestimated or that mycorrhizae and rhizodeposition became an increasingly important component of the C balance. Under elevated CO₂, net ecosystem production increased by 272 g C m⁻² a⁻¹: 44% greater than under ambient CO₂. The majority (87%) of this C was sequestered in a moderately long-term C pool in wood, with the remainder in the forest floor–soil subsystem.

Keywords: Canopy stomatal conductance, Free air CO₂ enrichment, net ecosystem exchange, net primary productivity, plant canopy modelling, respiration

Received 3 October 2002; revised version received 11 April 2003 and accepted 24 April 2003

Introduction

Attempting to reduce the rate at which atmospheric CO₂ increases, the Kyoto Protocol has transformed CO₂ emissions and sinks into valuable trading commodities (Steffen *et al.*, 1998). The size of the carbon (C) sink in terrestrial ecosystems and the contribution of different processes to its strength under current atmospheric concentrations are still uncertain (Schimel *et al.*, 2001). The uncertainty over the strength of the sink in a future CO₂-enriched world is even greater (Houghton, 1997).

For example, despite some down-regulation of photosynthetic rates (A_{net}) under elevated CO₂ (Rey & Jarvis, 1998; Jach & Ceulemans, 2000; Griffin *et al.*, 2001; Tissue *et al.*, 2001; Rogers & Ellsworth, 2002), CO₂ uptake of canopies is expected to increase. However, the amount of C stored in the biosphere does not necessarily increase with the assimilation of CO₂ in photosynthesis (Valentini *et al.*, 2000). Uncertainties in C balances hamper the establishment and implementation of policies aimed at regulating atmospheric CO₂ concentrations.

To reduce uncertainties in the C balances, studies often combine different approaches and methodologies to estimate C fluxes into and out of vegetation. The

Correspondence: Ram Oren. e-mail: ramoren@duke.edu

degree of confidence in these estimates is high when different methods produce similar results, thereby 'closing' the C budget for an ecosystem. For example, physiological and biophysical models of net canopy assimilation (A_{nC}) and respiration by plants and microorganisms (Collatz *et al.*, 1991; Leuning *et al.*, 1998; Wang & Leuning, 1998) can be compared to C balances estimated by eddy covariance, biomass-based estimates of net primary productivity (NPP) and chamber based estimates of respiration (Law *et al.*, 1999). Interestingly, the degree of closure in the C balance varies considerably among studies (Baldocchi *et al.*, 1996; Luo *et al.*, 1997; Law *et al.*, 2000). A lack of closure in the C balance for plants growing under ambient conditions of atmospheric CO₂ (CO₂^a) is particularly troubling when the ultimate goal is to estimate C balances under elevated atmospheric CO₂ (CO₂^e). The lack of closure in C balances under CO₂^e suggests an incomplete understanding of key processes (including missing or neglecting appreciable pools and fluxes), improper model parameterization, errors in measurements, or erroneous gap-filling methodologies. These problems may cause a greater lack of closure under CO₂^e with an impetus to search for an explanation where none is needed.

Only two free air CO₂ enrichment (FACE) experiments exist in maturing forests, providing data on forest response to elevated CO₂ in otherwise unaltered conditions. One experiment is in a pure stand of *Liquidambar styraciflua* L. (Norby *et al.*, 2001), and one in a planted stand of *Pinus taeda* L. that currently includes 48 woody species and a large number of species of herbaceous plants and vines (DeLucia *et al.*, 1999; Hamilton *et al.*, 2002). In both these experiments, the plot size precludes the use of eddy covariance to estimate biosphere-atmosphere water vapour and heat exchange under CO₂^e, and the method cannot be used to quantify CO₂ flux because large quantities of CO₂ are emitted with FACE technology. A C balance of the CO₂^e experimental plots can be assessed by comparing A_{nC} estimated from a physiological model with gross primary productivity (GPP) estimated from the summation of biomass production and respiration. Although a number of studies have focused on different components of the C budgets at these sites (DeLucia *et al.*, 1999; Luo *et al.*, 2001; Oren *et al.*, 2001; Norby *et al.*, 2001; Finzi *et al.*, 2002; Hamilton *et al.*, 2002), the C balance of either site has not yet been verified using a combination of different approaches.

In this study, we linked a leaf-level CO₂ assimilation model (Katul *et al.*, 2000) with light models (Campbell & Norman, 1998; Stenberg, 1998) and sap-flux-based canopy conductance (Köstner *et al.*, 1992; Ewers & Oren, 2000) into a canopy-level model, hereafter

referred to as the canopy conductance-constrained CO₂ assimilation or 4C-A model. We tested the 4C-A model estimates of net photosynthesis (A_{net}) against leaf gas exchange measurements under ambient and elevated CO₂. Under CO₂^e we modelled net canopy assimilation (A_{nC}) and tested its prediction against independent measurements of net ecosystem exchange (NEE) and net ecosystem production (NEP), after accounting for respiration. We then used the model to assess the effect of CO₂^e on C uptake and allocation to different components of the C budget. Unlike other ecophysiological models (e.g. Leuning, 1995; Lai *et al.*, 2000; Baldocchi & Meyers, 1998), the 4C-A model is unique in that it uses nearly continuous measurements of canopy conductance to constrain CO₂ uptake by different species under varying environmental conditions. This approach eliminates the uncertainties that typically affect modelled stomatal conductance, but retains the biochemical processes necessary to estimate intercellular CO₂.

Material and methods

Study site

The site is located in Duke Forest, North Carolina, USA (35°58'N, 79°05'W). The average annual temperature is 15.5 °C and the annual precipitation is 1140 mm. The soil is a moderately well-drained low-fertility acidic Hapludalf of the Enon Series with a clay pan at ca. 30 cm depth. The even-aged *P. taeda* L. forest was planted in a clear-cut opening in 1983, with additional tree species representing seed sources of pine and broadleaf species from the surrounding area. The main broadleaf species are *L. styraciflua* L., *Acer rubrum* L., *Ulmus alata* Michx., and *Cornus florida* L. Further details about the site can be found in Ellsworth (1999) and Schäfer *et al.* (2002). The FACE facility at Duke Forest (Hendrey *et al.*, 1999) was designed with six circular plots (30 m in diameter), three of which are under CO₂^a and three under CO₂^e (ambient + 200 µmol⁻¹ CO₂ mol⁻¹ air). Radial boardwalks oriented in north-to-south and east-to-west directions transverse each plot.

Approach

We estimated canopy-level net daytime CO₂ uptake (in g C m⁻² ground s⁻¹) based on the 4C-A model. Sap-flux-based conductance estimates were available for a 1.5 m wide strip on each side of the boardwalk (211 m² of a plot total of 707 m²), and thus we applied our estimates to this section only in each plot. We first verified our A_{nC} estimate for ambient plot 1 against

the sum of daytime values of (1) CO₂ uptake from the atmosphere measured with eddy covariance above the canopy in this plot (F_C^a ; Lai *et al.*, 2000), (2) respiration estimated based on temperature-respiration functions for the forest floor (F_C^f) and above-ground woody biomass (maintenance respiration, R_M , and construction respiration, R_C), and (3) CO₂ depletion in the forest air volume from measurement of the CO₂ concentration profile between the forest floor and the position of the eddy-covariance system (ΔS_C^a). Following this verification step, we proceeded with a C balance, comparing the estimated A_{nc} for each plot with the sum of the annual utilization of C for growth, growth respiration, and maintenance respiration of the major biomass components.

In the following sections we describe the components of the 4C-A model, the set of independent measured fluxes obtained for verifying it under ambient conditions, and then the measurements obtained for balancing its A_{nc} estimates against growth and respiration under both ambient and elevated CO₂ atmosphere.

Modelling

At the leaf scale, net assimilation (A_{net} in $\mu\text{mol CO}_2 \text{ m}^{-2}$ projected leaf s^{-1}) and stomatal conductance are related as follows (Katul *et al.* 2000):

$$A_{net} = g_{\text{CO}_2} c_a \left(1 - \frac{c_i}{c_a} \right). \quad (1)$$

where c_a is external CO₂ concentration in $\mu\text{mol mol}^{-2}$, c_i is the internal CO₂ concentration in $\mu\text{mol mol}^{-1}$, and g_{CO_2} is mean stomatal conductance to CO₂ (mol m^{-2} leaf s^{-1}), calculated from mean stomatal conductance of water vapour corrected for the ratio of diffusivity of water vapour to CO₂ (1.6) assuming Fickian diffusion (for parameters, symbols, and units, see Table 1).

'Big-leaf' models that use a single canopy layer tend to underestimate A_{nc} due to non-linearity of the response to light of several photosynthetic processes (DePury & Farquhar, 1997; Friend, 2001). Thus, in order to estimate g_{CO_2} and C_i/C_a for calculating A_{nc} , we estimated the light regime in each of 16 1 m layers in the canopy and used this light as an input in modelling g_{CO_2} and C_i/C_a . There are several reasons as to why this approach is advantageous: (1) the integrated value of C_i/C_a from leaf to canopy is properly weighed by the conductance thereby resolving the interaction between C_i/C_a and g_{CO_2} while preserving the bulk canopy conductance; (2) variability in c_a across the canopy height can be explicitly incorporated in the up-scaling of C_i/C_a ; and (3) the physiological calculations are applied at the appropriate scale (i.e. leaf) prior to integration to the canopy level. In addition, modelled

long-term mean C_i/C_a can be tested against an independent estimate from $\delta^{13}\text{C}$ measurements.

Estimating the vertical profile of PPFD

The approach for estimating photosynthetic photon flux density ($PPFD$ in $\mu\text{mol m}^{-2} \text{ s}^{-1}$) at each layer in the canopy, and the proportion of foliage receiving different quantities of $PPFD$ at each layer is described in the Appendix. Briefly: (1) incoming $PPFD$ was partitioned into direct and diffuse components (Erbs *et al.*, 1982), (2) the seasonal dynamics of leaf area density profile was modelled separately for the *P. taeda* (Kinerson *et al.*, 1974; Pataki *et al.*, 1998) and deciduous broadleaf species, (3) $PPFD$ was estimated in each layer at half-hourly intervals, accounting for direct and diffuse components, using the penumbral effect to partition the direct component into 10 light categories (Campbell & Norman, 1998; Stenberg, 1998), and (4) the proportion of foliage in each light category was estimated (Campbell & Norman, 1998; Stenberg, 1998).

In coniferous stands, penumbral effects redistribute direct light, enhancing photosynthesis of the more shaded foliage. During periods of high light this redistribution of direct light occurs without impact on the oversaturated sunlit foliage. The model calculates the proportion of leaf area for which direct beam radiation is obstructed by 0, 1, ..., 9 branches in each canopy layer, and the light intensity incident on the leaf surface in each of the 10 light categories. To the light intensity thus calculated, the amount of diffuse and scattered light is added, producing half-hourly estimates of total incident $PPFD$ in each category. In summary, the model explicitly resolves the seasonal dynamics of leaf area profile and its effect on the entire light environment (and thus the canopy-integrated C_i/C_a).

The ultimate goal of assembling this model is to estimate A_{nc} under CO₂. Recent findings on *P. taeda* in this site showed that previous-year foliage in CO₂ plots has 75% the carboxylation capacity of that in CO₂ plots (Rogers & Ellsworth, 2002) and current-year foliage has ~90% that in CO₂ plots. We therefore accounted for the vertical distribution of current- and previous-year foliage by 'growing' the canopy in relation to the vertical pattern of seasonal needle elongation (see the Appendix).

Estimating the vertical profile of stomatal conductance

We employed the following approach to estimate stomatal conductance in leaves positioned along the canopy: (1) $PPFD$ was calculated for each category at half-hourly intervals at each layer and combined with stomatal conductance- $PPFD$ response functions of sun-type and shade-type foliage derived from leaf gas exchange measurements (CIRAS-1, PP-systems, Ellsworth, 1999, 2000; Naumburg & Ellsworth, 2000) to

Table 1 Parameters and their definition used in the model

Parameter	Definition	Unit
C_i/C_a	Long-term mean C_i/C_a based on $\delta^{13}\text{C}$	Dimensionless
β	Silhouette to leaf area ratio	Dimensionless
H	Clumping factor	Dimensionless
ρ	Density of water at 4 °C	998 kg m ⁻³
κ	Zenith angle	
Γ^*	CO ₂ compensation point	μmol mol ⁻¹
τ_b	Light transmission coefficient for direct radiation	Dimensionless
τ_d	Light transmission coefficient for diffuse radiation	Dimensionless
τ_s	Light transmission coefficient for scattered radiation	Dimensionless
z_p	Leaf absorptivity of PPFD	Dimensionless
ΔS_C^a	Change in atmospheric CO ₂ storage in forest air volume	g C m ⁻² ground s ⁻¹
a, b, s, y_0	Fitting parameters	
A_{nC}	Canopy net assimilation	μmol m ⁻² ground s ⁻¹
A_{net}	Leaf net assimilation	μmol m ⁻² leaf s ⁻¹
B_S	Standing biomass	g C m ⁻² ground a ⁻¹
c	Transmission coefficient	Dimensionless
c_a	Atmospheric CO ₂ concentration	μmol mol ⁻¹
CE	Carboxylation efficiency	
CE_{max}	Maximum light saturated CE	μmol m ⁻² s ⁻¹
c_i	Substomatal cavity CO ₂ concentration	μmol mol ⁻¹
D	Water vapour pressure deficit of air	kPa
DIC	Dissolved inorganic carbon	g C m ⁻² ground a ⁻¹
DOC	Dissolved organic carbon	g C m ⁻² ground a ⁻¹
E_C	Canopy transpiration	mmol m ⁻² ground a ⁻¹
E_L	Canopy transpiration per unit leaf area	mmol m ⁻² leaf s ⁻¹
F_C^a	Atmospheric CO ₂ flux	g C m ⁻² ground s ⁻¹
F_C^{ff}	Forest floor CO ₂ efflux	μmol m ⁻² s ⁻¹
f_{st}	Sunlit fraction of foliage	
g_{CO_2}	Leaf-level stomatal conductance to CO ₂	mol m ⁻² leaf s ⁻¹
g_{crit}	Critical conductance	mol m ⁻² leaf s ⁻¹
GPP	Gross primary productivity	g C m ⁻² ground s ⁻¹
G_S	Canopy stomatal conductance to water vapor	mmol m ⁻² leaf s ⁻¹
G_{SCO_2}	Canopy stomatal conductance to CO ₂	mmol m ⁻² leaf s ⁻¹
g_{sh}	Stomatal conductance to CO ₂ for shaded foliage	mol m ⁻² leaf s ⁻¹
g	Stomatal conductance to CO ₂ for sunlit foliage	mol m ⁻² leaf s ⁻¹
G_{Sref}	Reference G_S at 1 kPa	mmol m ⁻² leaf s ⁻¹
G_V	Universal gas constant corrected for water vapour	0.462 kPa m ³ K ⁻¹ kg ⁻¹
I_b	Direct radiation	μmol m ⁻² ground s ⁻¹
I_{bi}	Direct radiation in layer i	μmol m ⁻² ground s ⁻¹
I_C	Light compensation point	μmol m ⁻² ground s ⁻¹
I_d	Diffuse radiation	μmol m ⁻² ground s ⁻¹
I_{di}	Diffuse radiation in layer i	μmol m ⁻² ground s ⁻¹
I_{ex}	Extraterrestrial radiation	μmol m ⁻² ground s ⁻¹
I_o	Total incoming radiation	μmol m ⁻² ground s ⁻¹
I_{sc}	Scattered radiation in layer i	
I_S	Light saturation point	μmol m ⁻² ground s ⁻¹
k	Probability of light category (for <i>P. taeda</i>)	
K_{be}	Light extinction coefficient for direct radiation	Dimensionless
K_d	Light extinction coefficient for diffuse radiation	Dimensionless
K_T	Clearness index	Dimensionless
L	Leaf area index	m ² m ⁻²
LOC	Lack of closure	
L_t	Leaf area density	m ² m ⁻²
L_{ti}	Cumulative leaf area density in layer i	
M_0, x_0	Fitting parameter	

Table 1 (Continued)

Parameter	Definition	Unit
N	Nitrogen concentration	$\mu\text{mol mol}^{-1}$
NEE	Net ecosystem exchange	$\text{g C m}^{-2} \text{ground s}^{-1}$
NEP	Net ecosystem productivity	$\text{g C m}^{-2} \text{ground a}^{-1}$
NPP	Net primary productivity	$\text{g C m}^{-2} \text{ground a}^{-1}$
$PPFD$	Photosynthetic photon flux density	$\mu\text{mol m}^{-2} \text{ground s}^{-1}$
R_A	Autotrophic respiration	$\text{g C m}^{-2} \text{ground s}^{-1}$
R_C	Construction respiration	$\text{g C m}^{-2} \text{ground s}^{-1}$
R_E	Ecosystem respiration	$\text{g C m}^{-2} \text{ground s}^{-1}$
R_H	Heterotrophic respiration	$\text{g C m}^{-2} \text{ground s}^{-1}$
R_M	Maintenance respiration	$\text{g C m}^{-2} \text{ground s}^{-1}$
T_a	Air temperature	$^{\circ}\text{C}$
T_{stem}	Stem temperature	$^{\circ}\text{C}$
V_{cmax}	Maximum RubisCO capacity	$\mu\text{mol m}^{-2} \text{leaf s}^{-1}$
x	Leaf angle distribution	Dimensionless

estimate conductance. Shade-type foliage was foliage exposed to direct light less than 35% of the time. (2) Stomatal conductance was scaled to the layer based on L of each foliage type in each $PPFD$ category, summed for all layers, and expressed as the relative contribution of stomatal conductance in each type within each layer to that of the total canopy. (3) Relative conductance was multiplied by the sap-flux-scaled canopy stomatal conductance (G_S), repartitioning G_S between foliage types among layers.

Over the 3 years in which A_{nc} was estimated based on the 4C-A model, sap flux-scaled conductance was available for 55 991 (i.e. 86% recovery) half-hourly daytime values for *P. taeda*, and 28 603 (65%) for the hardwoods. Many of the missing data (~80%) represent conditions in which G_S calculated from sap-flux measurements incur large error (i.e. $D < 0.6$ kPa, based on Ewers & Oren, 2000). The remaining proportion of missing data represents instrument or power failure, or when hardwoods are not in leaf.

Estimating the ratio of internal-to-external CO_2 concentration

The ratio of CO_2 concentration in the stomatal cavity relative to the concentration at the leaf surface (c_i/c_a) can be modelled after Katul *et al.* (2000). The c_i/c_a was calculated separately for $PPFD < I_S$ and $PPFD > I_S$ where I_S is the light saturation point of the mean leaf carboxylation efficiency (CE), considering CE as the initial slope of the $A_{\text{net}} - c_i$ curve. Under conditions of $PPFD \geq I_S$, c_i/c_a was calculated separately for g_{CO_2} less than a critical conductance (g_{crit}) and for $g_{\text{CO}_2} \geq g_{\text{crit}}$ *stm*. Critical conductance is the conductance in which c_i reaches sufficiently high values so $\delta A_{\text{net}}/\delta g_{\text{CO}_2} \rightarrow 0$. The critical conductance is calculated based on Katul

et al. (2000) as

$$g_{\text{crit}} = \frac{CE \times \overline{c_i/c_a} - (CE \times \Gamma^*)/c_a}{1 - \overline{c_i/c_a}} \quad (2)$$

where Γ^* is the CO_2 compensation point (not considering mitochondrial respiration) calculated from the $A_{\text{net}} - c_i$ curve measured *via* leaf gas exchange measurements (Ellsworth 1999, 2000, Herrick & Thomas 1999, 2001), and $\overline{c_i/c_a}$ is the long-term mean C_i/C_a ratio obtained from $\delta^{13}\text{C}$ measurements. Although this approach describes the biochemical processes less realistically than models based on Farquhar *et al.* (1980), it preserves the key biochemical mechanisms linking c_i to A_{net} . Furthermore, the uncertainty added with increasing numbers of model parameters can degrade performance when compared to leaf gas exchange measurements (Katul *et al.*, 2000), a factor that is likely to be particularly troublesome in studies aimed at long-term estimates of gas exchange.

Thus, for conditions in which $PPFD < I_S$, or $PPFD \geq I_S$ and $g_{\text{CO}_2} < g_{\text{crit}}$,

$$\frac{c_i}{c_a} = \frac{g_{\text{CO}_2} + (CE \times \Gamma^*)/c_a}{CE + g_{\text{CO}_2}} \quad (3)$$

The c_i/c_a can be estimated from this relationship when the $A_{\text{net}} - c_i$ curve is approximately linear for the range of external CO_2 concentration. This condition was satisfied for both sun- and shade-type foliage initiated under both CO_2^{a} and CO_2^{s} in our stand (Ellsworth, 1999; Herrick & Thomas, 2001). For conditions in which $g_{\text{CO}_2} \geq g_{\text{crit}}$, g_{CO_2} is set to equal g_{crit} , and c_i/c_a is calculated based on Eqn (3).

The Γ^* in Eqns (2) and (3) is similar in a large variety of C_3 species and environmental conditions; thus, a single base value may be used for both *P. taeda* and the broadleaf species vertically through the canopy (Wilson

et al., 2000). The base value of I^* is corrected for temperature based on Katul *et al.* (2000). In contrast, maximum CE (CE_{\max}) is 75% higher in sun- than in shade-type foliage, increases with *PPFD*, and shows seasonal dynamics that approximately reflects the changing temperature.

In each foliage type of *P. taeda*, the maximum carboxylation capacity ($V_{C_{\max}}$), measured *via* leaf gas exchange under saturating light conditions, has a distinctly large seasonal course deviating ~20% above and below the annual mean (Ellsworth, 2000). The seasonal course is just as pronounced in the foliage of some deciduous broadleaf species, with a pattern resembling that of *L* (Wilson *et al.*, 2000). The seasonal dynamics in CE_{\max} is primarily driven by the dynamics in $V_{C_{\max}}$, because both are fitted to the actual or to the temperature and kinetic coefficient-corrected relationship between A_{net} and c_i :

$$\begin{aligned} \text{in } P. \text{ taeda foliage : } CE_{\max} &= 0.4716 \\ &\times \log(0.00249 \times (V_{C_{\max}}) \\ &+ 0.9915), \end{aligned} \quad (4)$$

$$\begin{aligned} \text{in } L. \text{ styraciflua foliage : } CE_{\max} &= 0.00079 \\ &\times (V_{C_{\max}}) + 0.0099. \end{aligned} \quad (5)$$

We approximated the seasonal dynamics of CE_{\max} for *P. taeda* using a sine wave function with minima (0.8 of the long-term mean; see the mean in Table 2) in January 31 and maxima (1.2 of the mean) in July 31, approximately at the time of year in which temperature minima and maxima occurred during the study (Schäfer *et al.*, 2002). The CE_{\max} for the hardwood species after bud break was set to 0.1 of the maximum value obtained in June (Herrick & Thomas, 2001), increasing to the maximum in June and decreasing to 0 thereafter with the entire dynamics set to mimic that of *L*. CE_{\max} is discounted to actual CE by accounting for the incident *PPFD*. Thus, CE was set to zero at the photosynthetic light compensation point (I_C) of each species (Table 2), increasing linearly with *PPFD* until CE_{\max} is reached at the point in which photosynthetic rate was nearly saturated with respect to light (I_S ; Table 2). Any further increase in photosynthesis with $PPFD > I_S$ is related to an increase in g_{CO_2} with light.

For the shade-type foliage of the broadleaf species, we used the leaf-area-weighted mean of the physiological parameters of four species measured at the site, including the dominant broadleaf species *L. styraciflua* (Naumburg & Ellsworth, 2000). Broadleaf sun-type foliage was almost exclusively *L. styraciflua*, for which we used locally measured parameters (Herrick & Thomas, 2001).

Table 2 Parameters (mean and standard error in parenthesis) used for calculating canopy net assimilation and respiration under ambient (CO₂) and elevated (CO₂^e) conditions

		<i>Pinus taeda</i>		<i>Liquidambar styraciflua</i>	
		Sun	Shade	Sun	Shade
<i>Leaf</i>					
β		0.5			1.0
z_p				0.83	
c		0.4			Not applicable
<i>H</i>					
CE_{\max}	CO ₂	0.07 (0.002)	0.04	0.062	0.035 (0.0003)*
	CO ₂ ^e	0.07† (0.002)	0.04†	0.062	0.033 (0.0012)*
		0.05‡ (0.002)	0.03‡		
$\overline{C_i/C_a}$	CO ₂			0.69 (0.01)	
	CO ₂ ^e	0.68 (0.02)	0.77 (0.01)	0.65 (0.02)	
I_S		700	400	700	400
I_C		35	20	27	15
<i>Wood</i>					
N	CO ₂	Branch 2.3 (0.3)	Stem 0.95 (0.04)	Branch 4.0	Stem 1.8
	CO ₂ ^e	2.1 (0.1)	0.89 (0.07)	3.0	1.4

Parameter values of *L. styraciflua* are provided because this species dominated the broadleaf component at the site. Parameters definitions and units are provided in Table 1. Centred values represent both foliage types or both species.

*Leaf area weighted CE for four species that were measured; see text for details.

†Current-year foliage.

‡Previous-year foliage.

The effect of CO₂^e on CE_{\max} was accounted for by a change proportional to that observed in $V_{C_{\max}}$. For *P. taeda*, a reduction in CE_{\max} for previous-year foliage was 25% (Rogers & Ellsworth, 2002) and for current-year foliage up to 10%. This effect was captured through a linear reduction in CE_{\max} for current-year foliage beginning at the initiation of needle elongation, reaching 10% when needle elongation of all flushes is completed, and remaining at this level until the end of the year, at which point the now previous-year foliage decreases linearly, reaching the 25% mark by the time of bud break and remaining at this level until senescence. For the broadleaf species the effect of CO₂^e on CE_{\max} was not significant in most studies (Herrick & Thomas, 1999; Naumburg & Ellsworth, 2000), but has recently

been shown to cause an ~13% reduction in CE_{\max} for *L. styraciflua* (Ellsworth, unpublished).

Estimating canopy net assimilation

The net assimilation rate per unit of leaf surface ($\text{mmol m}^{-2} \text{leaf s}^{-1}$) calculated according to Eqn (1) in each light category was scaled to canopy A_{nC} using the leaf area in each category ($\text{g m}^{-2} \text{ground}^{-1} \text{s}^{-1}$). A_{nC} was summed across all light categories in each canopy layer for each species, and was then expressed for each species type or for the entire canopy.

Measurements

Measurements of sap flux and environmental variables

Sap flux (Granier, 1987) and environmental variables used in calculating and modelling G_S were measured continuously in each plot from May 1997 to December 2000. Detailed information on sampling, calculations, and modelling are provided in Schäfer *et al.* (2002, in review). Of special relevance to this study, *PPFD* was measured with a sensor mounted to the central tower above the canopy of one plot (Q190, LiCor, Lincoln, NE, USA). Stem temperature (T_{stem} in °C) in four cardinal directions was measured in one tree and on the north side of two additional trees, soil temperature was measured at 10–15 cm depth at each plot (M 841/S1, Siemens, Germany) and air temperature (T_a in °C) was also measured in each plot at two-thirds of the height of the canopy (Vaisala HMP35C or HMP45C, Helsinki, Finland). These temperature measurements were used to estimate R_M and F_C^{ff} (Maier *et al.* 1998, Butnor *et al.*, 2003). All measurements were sampled every 30 s and 30 min averages were stored in a data logger (21X or 23X, Campbell Scientific, Logan, UT, USA).

Estimating biomass production and respiration components

Based on previous studies, it was assumed that allometric relationships are not affected by elevated CO_2 (Norby *et al.*, 2001; Pataki *et al.*, 1998; DeLucia *et al.*, 2002), justifying the use of the same relationship under ambient and elevated CO_2 conditions. We further verified that allometry is not altered by growth under CO_2^{s} by measuring height and diameter of *Pinus taeda* ($n = 121$ under CO_2^{s} and 102 under CO_2^{a}), *Liquidambar styraciflua* ($n = 53$ and 66), *Cornus florida* ($n = 20$ and 12), and *Ulmus alata* ($n = 39$ and 34) trees; the relationship of height and diameter at 1.4 m above ground did not differ between the treatments for any species (minimum $P > 0.3$).

Broadleaf individuals 12–125 mm in diameter at 1.4 m above ground were harvested in 1998 and 1999 in order to develop allometric equations for estimating L , L profile, and above-ground biomass components of the

prevailing broadleaf species in the stand. The individuals were harvested in the stand but outside of the experimental plots. The species were *Lirodendron tulipifera* (seven individuals), *A. rubrum* (seven; Naumburg & Ellsworth, 2000), *L. styraciflua* (15), *C. florida* (10), and, *U. alata* (7; Schäfer *et al.*, in review), species comprising 48–98% of the broadleaf basal area in the six experimental plots. For *P. taeda*, allometric equations were available for the site (Naidu *et al.*, 1998; Pataki *et al.*, 1998).

For the broadleaf species, harvest date was timed to the period of full leaf expansion, after stem growth was mostly completed, and before leaf senescence. After cutting at ground level, the height, base of crown, position of each branch along the stem, and its diameter were recorded. Then, the biomass was partitioned into leaf, branches and stem-components, dried (wholly for individuals <45 mm, or subsampled, 1 week; 80 °C), and weighed. Specific leaf area was determined on a subset of leaves from each branch (individuals <45 mm) or every third branch (larger individuals). A relationship of sapwood-to-leaf area ratio vs. diameter at 1.4 m (Schäfer *et al.*, in review) was generated for each species. Standing biomass of each component was estimated from diameter measured on all trees in the measurement plots in November of each year (1998–2000), and the allometric relationships with diameter derived from biomass harvests. The biomass and leaf area of each species in the study for which allometric relationships were not developed at the site were estimated based on relationships developed for the species with the closest resemblance.

For *P. taeda*, estimates of stem, branch, and root biomass were based on Naidu *et al.* (1998), and needle biomass and area were based on Pataki *et al.* (1998). *P. taeda* comprise at least 80% of the basal area in each measurement plot.

NPP was calculated as the difference of current- to previous-year standing biomass augmented with fine root turnover (Matamala & Schlesinger, 2000). To this value we added litterfall of *P. taeda* (Finzi *et al.*, 2001), representing needle turnover, and the estimated leaf biomass produced by the broadleaf species.

To estimate maintenance respiration of branches and stems (R_M), standing biomass was incremented reflecting the stem growth dynamics (Oren *et al.*, 2001), and R_M was estimated based on the biomass, stem temperature and nitrogen concentration (see Table 2) after Maier *et al.* (1998) and Maier (2001). Maintenance respiration of coarse roots was calculated based on soil temperature, nitrogen content, and root biomass (Maier, unpublished results). Maintenance respiration of foliage, calculated only over night-time hours, was estimated using air temperature as a proxy of leaf

temperature, assuming the canopy is well coupled (Phillips *et al.* 1997), based on relationships developed on site under each CO₂ treatment for *P. taeda* and *L. styraciflua*, the latter being used as a surrogate for all other broadleaf species (Hamilton *et al.*, 2001). Fine root respiration was taken from previously published values of Matamala & Schlesinger (2000).

Construction respiration was calculated for each organ separately. The construction cost of stems and branches of all species is similar (Wullschleger *et al.*, 1997; Hamilton *et al.*, 2002), and is not affected by atmospheric CO₂ concentration (Carey *et al.*, 1996). Thus, the construction cost for these organs was taken as 1.50 g glucose g⁻¹ dry weight of constructed tissue (Carey *et al.* 1996). Construction respiration of coarse roots was estimated using 1.47 g glucose g⁻¹ dry weight (Maier, unpublished results), assuming no difference among species and CO₂ treatments. The construction cost of *P. taeda* needles was estimated using 1.45 g glucose g⁻¹ dry weight for both CO₂ treatments (Griffin *et al.*, 1993, 1996; Hamilton *et al.*, 2001). However, there is evidence that construction respiration for the hardwood leaves increased under CO₂ from 1.41 g glucose g⁻¹ dry weight under CO₂ to 1.46 g glucose g⁻¹ dry weight for leaves produced under CO₂ (Wullschleger *et al.*, 1997).

Unless otherwise stated, data were analysed based on a paired *t*-test (*n* = 3) with plot paired according to sapwood area per unit of ground area (Schäfer *et al.*, 2002).

Results

Model evaluation

The c_i/c_a as a function of varying PPFD alone or together with g_{CO_2} is shown for sun- and shade-type foliage of the two main species (Fig. 1c,d), along with their g_s (Fig. 1a,b) and estimated leaf level A_{net} (Fig. 1e,f). The 4C-A model reproduced the expected pattern of responses of c_i/c_a and A_{net} to light, and a number of additional responses to g_s , D , and θ (data not shown). The canopy-level 4C-A model reproduced the expected corresponding patterns in A_{nC} (Fig. 1g,h). As shown for 1999, the model produced a spatio-temporal light pattern (Fig. 2b) that captured both the dynamics in L (Fig. 2a) and in incoming light, influenced by the sun angle and clouds, and especially by the ephemeral pattern of the broadleaf foliage (Fig. 2a). The seasonal and vertical patterns in A_{nC} (Fig. 2c) reflect the dynamics in incoming light and L , and the effect of CO₂ is discernible (Fig. 2d). Day-to-day variations in light due to clouds are clearly reflected in the vertical pattern of A_{nC} . The vertical pattern of A_{nC} shows the relative little contribution of the broadleaf

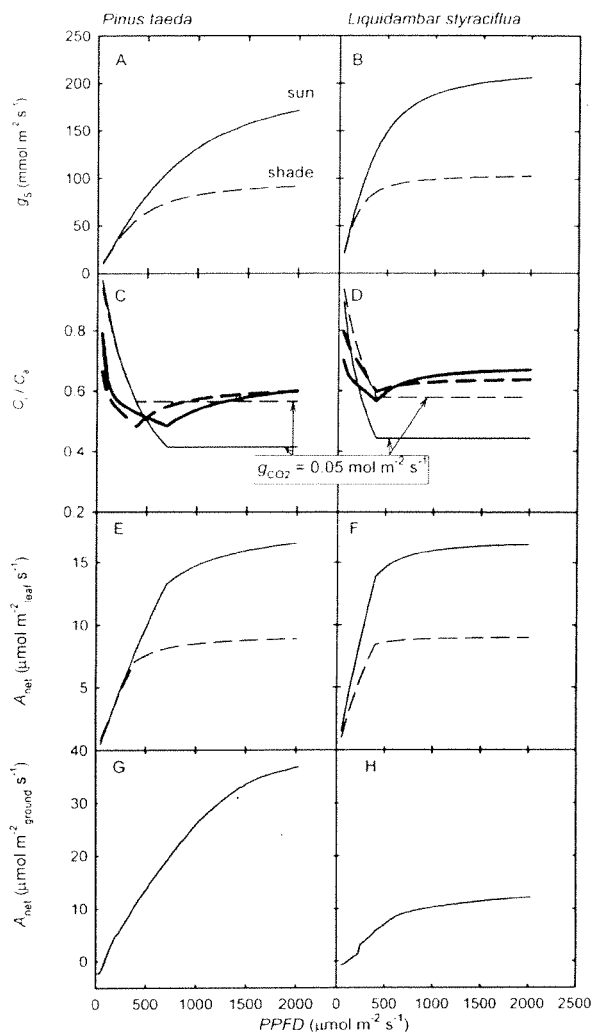


Fig. 1 Modelled responses of stomatal conductance (g_s , a and b), ratio of leaf internal to external atmospheric CO₂ concentration (c_i/c_a , c and d), leaf net assimilation (A_{net} , e and f), and canopy net assimilation (A_{nC} , g and h) vs. light (PPFD) for the canopy dominant species *P. taeda* (a, c, e, and g) and the most abundant broadleaf species *L. styraciflua* (b, d, f, and h) at the Duke Forest site.

species to the total canopy photosynthesis, and the high contribution of *P. taeda*, especially during the period in which the sun angle is steepest.

The ecosystem net assimilation estimate was first evaluated under ambient conditions by comparing it with: (1) with daytime net ecosystem exchange (F_e^D) measured *via* eddy covariance over the entire canopy of an ambient plot, augmented with daytime forest floor CO₂ flux (F_C^D) and above-ground construction and maintenance respiration (R_M and R_C), with construction respiration assumed to be one half the daily estimate, and with the change in CO₂ storage in the forest air

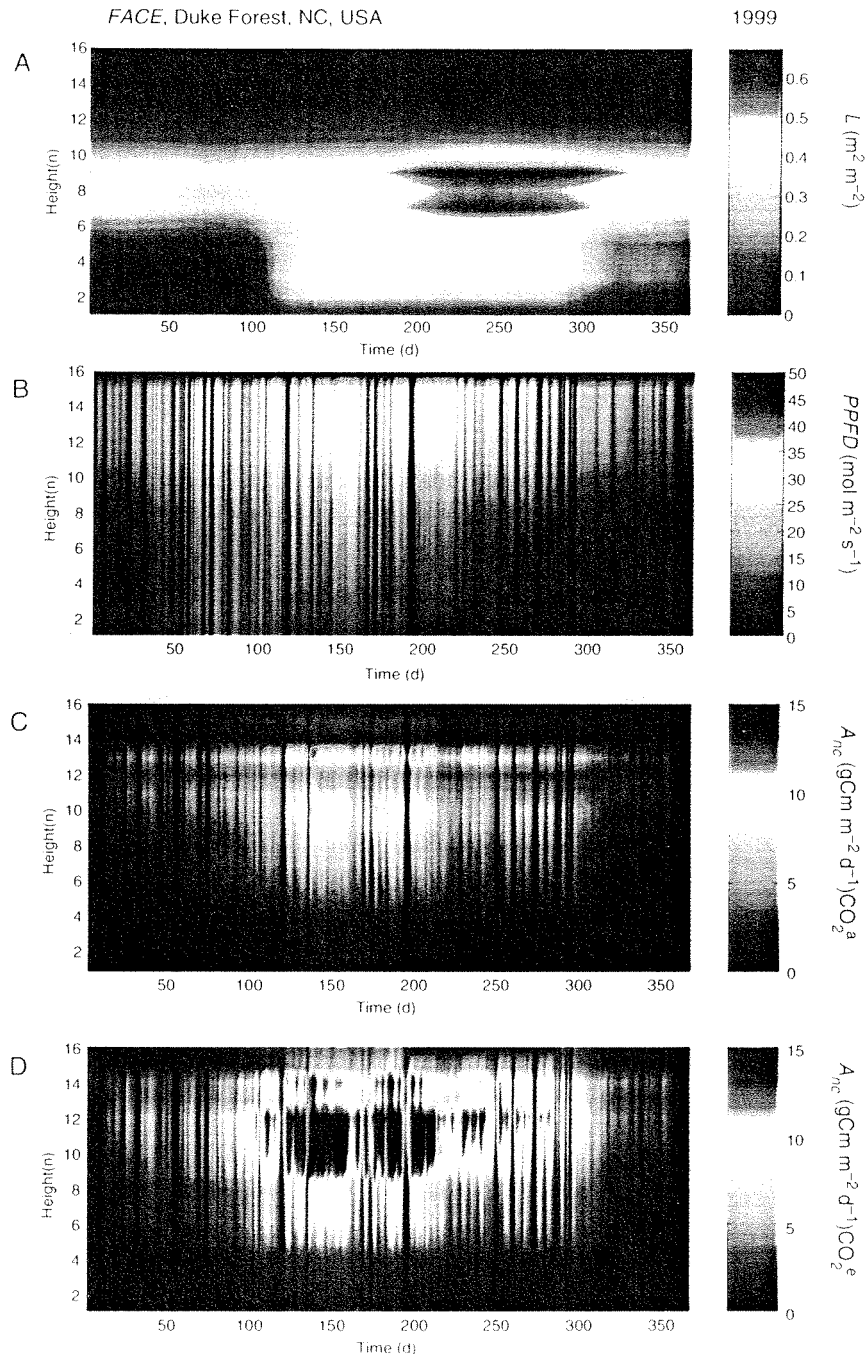


Fig. 2 Daily values for 1999 of vertical distribution in the canopy for (a) mean leaf area index (L), (b) integrated light ($PPFD$), (c) integrated canopy net assimilation (A_{net}) averaged for ambient plots (CO_2^a), and (d) integrated A_{net} averaged for elevated plots (CO_2^e).

volume (ΔS_C^2) (Lai *et al.* 2000); (2) NPP estimates derived from allometric relationships augmented with whole plant maintenance (R_M) and construction respiration (R_C); and (3) instantaneous measurements of A_{net} at the upper third of the canopy *via* leaf gas exchange measurements under both CO_2^a and CO_2^e .

Reliable estimates of net ecosystem exchange (24 h, NEE) were available for 37 of the months from August 1997 to December 2000 (Fig. 3a). For the same period we show the seasonal dynamics of the estimated values of R_M and R_C , A_{net} , combined for broadleaf and *P. taeda*, and F_C^{ff} (Fig. 3b–e). We note that the period in which A_{net}

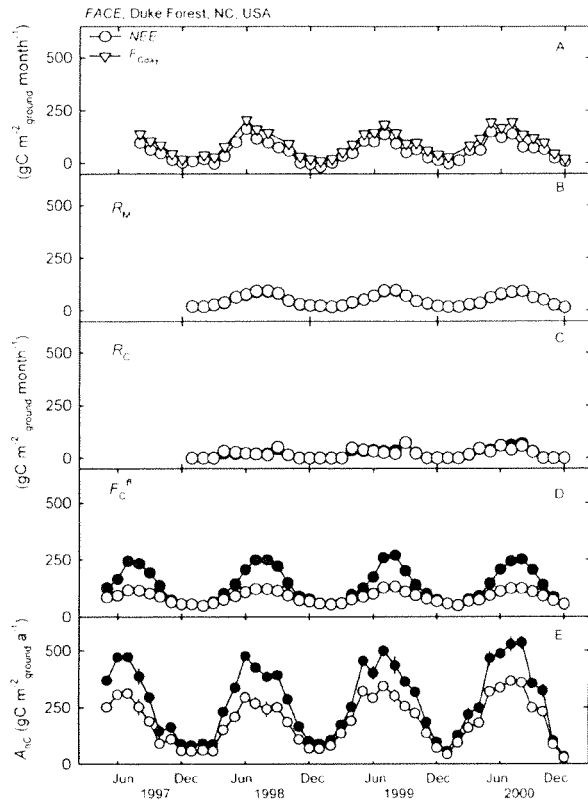


Fig. 3 Monthly fluxes throughout the study period of (a) net ecosystem exchange (F_C , open circles) and net ecosystem exchange for daytime only ($F_{C,day}$, open triangles) for ambient CO₂ only, (b) maintenance respiration (R_M) summed for woody components, roots, leaves, and needles, (c) construction respiration (R_C) summed for woody components, roots, leaves, and needles, (d) forest floor CO₂ efflux (F_C^{ff}), and (e) canopy net assimilation (A_{nC}) under ambient (open symbols) and elevated (filled symbols) conditions. Where filled symbols are not seen, they are obstructed by open symbols.

is highest occurs 2 months before L reaches its maximum late in the season (Phillips & Oren, 2001), and result in that maintenance and construction respiration reaching their highest values while A_{nC} is already decreasing (Fig. 3b,c and e). The most noticeable patterns are the relative invariance of the annual course of all respiration components, and the progressive increase in the maximum monthly value of A_{nC} during the experiment, reflecting mostly the increase in L .

We tested the 4C-A model skill by comparing A_{nC} against the balance of fluxes measured or calculated for the site. The monthly estimates of A_{nC} were higher than the sum of the contributing flux components (Fig. 4a). Modelled A_{nC} summed for each month showed a clear positive bias, averaging about 13% higher than the contributing components in the 3 years with sufficient data, with the worst annual agreement of 29% in 1999,

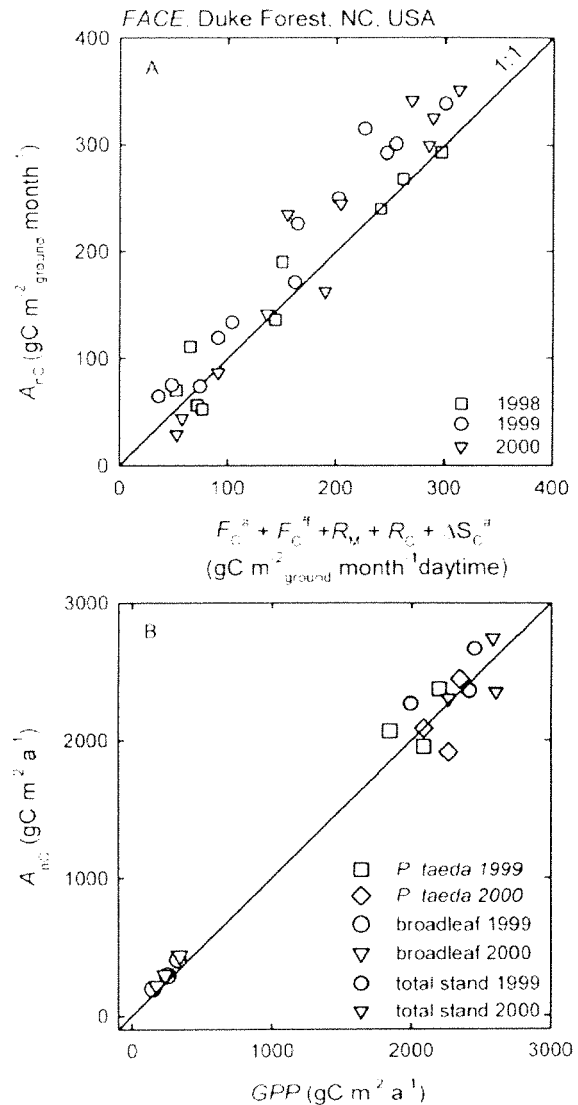


Fig. 4 (a) Monthly flux comparison of net canopy assimilation (A_{nC}) vs. the sum of contributing components during daytime: net ecosystem exchange (F_C^a), forest floor CO₂ efflux (F_C^{ff}), maintenance respiration of woody biomass during daytime (R_M), construction respiration (R_C), and change in CO₂ storage in the forest air volume (ΔS_C^d). (b) Comparison of A_{nC} vs. gross primary production (not including daytime leaf respiration) on an annual basis for 1999 and 2000 for individual plots for the *P. taeda* component, the broadleaf canopy component, and for the combined canopy. The 1:1 line is also shown for reference. Both comparisons made ambient CO₂.

and a best of 4% in 2000 (Fig. 4a). We evaluated the effect of uncertainty in the least well-quantified parameters of the 4C-A model, the mean annual value of maximum light saturated CE_{max} and the light levels at which CE_{max} is set to zero or to the maximum, by changing each parameter $\pm 10\%$. Changing the mean annual $CE_{max} \pm 10\%$ causes a corresponding change of

Table 3 Components of the annual carbon balance (in $\text{g C m}^{-2} \text{a}^{-1}$) including net primary productivity, respiration, and estimates for canopy photosynthesis from the 4-CA model (A_{nC}) and from the sum of components (GPP). Bold type indicates differences significant at $P \leq 0.09$

	1999			2000		
	CO_2^a	CO_2^b	<i>P</i> value	CO_2^a	CO_2^b	<i>P</i> value
<i>P. taeda</i>						
Total R_M^*	1014 (71)	1036 (206)	0.93	1022 (78)	1060 (209)	0.88
Total R_C	204 (14)	250 (23)	0.07	241 (12)	296 (38)	0.17
Total NPP^{\ddagger}	825 (50)	1026 (101)	0.09	972 (37)	1207 (162)	0.19
<i>GPP</i>	2043 (105)	2312 (326)	0.45	2235 (77)	2563 (408)	0.47
A_{nC}	2131 (125)	2830 (278)	0.04	2148 (157)	2967 (299)	0.03
$A = A_{nC} - GPP$	88 (122)	518 (66)		- 86 (137)	404 (110)	
$A > 0, P =$	0.57	0.02		0.52	0.08	
<i>Hardwoods</i>						
Total R_M^*	137 (32)	184 (50)	0.18	137 (32)	184 (51)	0.17
Total R_C	22 (5)	25 (7)	0.35	25 (3)	26 (7)	0.84
Total NPP^{\ddagger}	84 (16)	101 (26)	0.23	89 (14)	106 (32)	0.44
<i>GPP</i>	244 (53)	310 (82)	0.19	252 (48)	316 (90)	0.27
A_{nC}	300 (60)	557 (241)	0.30	317 (65)	563 (239)	0.30
$A = A_{nC} - GPP$	56 (11)	247 (164)		66 (18)	246 (150)	
$A > 0, P =$	0.05	0.26		0.05	0.24	
<i>Stand</i>						
Total R_M^*	1152 (103)	1220 (89)	0.76	1160 (109)	1245 (190)	0.71
Total R_C	226 (15)	275 (19)	0.05	266 (10)	322 (33)	0.14
Total NPP^{\ddagger}	909 (54)	1127 (88)	0.06	1060 (25)	1313 (141)	0.15
<i>NEP</i> Ia§	488 (172)	185 (219)	0.34	669 (141)	397 (281)	0.47
<i>NEP</i> II§	576 (37)	872 (55)	0.02	654 (4)	1030 (106)	0.07
<i>NEE</i>	661			792		
<i>GPP</i>	2287 (148)	2622 (292)	0.32	2486 (110)	2879 (364)	0.36
A_{nC}	2431 (120)	3387 (160)	< 0.01	2466 (139)	3530 (212)	0.01
$A = A_{nC} - GPP$	144 (102)	765 (191)		- 20 (123)	651 (240)	
$A > 0, P =$	0.39	0.05		0.64	0.11	

The data are provided separately for *Pinus taeda* and for the broadleaf species, and summed to the stand level. Net ecosystem exchange (*NEE*) is given for the stand under CO_2^b only.

*Augmented with fine root respiration (Matamala & Schlesinger, 2000).

†Augmented with fine root increment (Matamala & Schlesinger, 2000).

‡Augmented with litter fall data (Finzi *et al.*, 2001).

§*NEPI* based on flux components ($NPP - R_{f1}$), and *NEP* II based on C pools; see text for details.

$\sim \pm 5\%$ in A_{nC} ($\pm 120 \text{ g m}^{-2} \text{ a}^{-1}$). Increasing and decreasing the light level at which $CE_{\max} = 0$ caused a -6% and $+1\%$ change in A_{nC} , respectively, while these changes in the light level at which CE_{\max} reaches its maximum value caused a -9% and $+4\%$ change in A_{nC} . Thus, the likely errors in parameter values used in the 4C-A model runs would not reduce A_{nC} sufficiently to match the estimates based on the sum of flux components (Fig. 4a).

On an annual basis, A_{nC} under CO_2^b balanced well with the sum of NPP , R_C and R_M (i.e. GPP , not including daytime leaf respiration) for both *P. taeda* and the broadleaf species, and for their sum (Fig. 4b; Table 3).

Averaged for the 2 years, A_{nC} in CO_2^b was 3% more than GPP . Using a constant C_i/C_a for each foliage type (after Norman 1982) but keeping the conductance as in the 4C-A model resulted in $\sim 20\%$ higher A_{nC} than that estimated with 4C-A, while a big-leaf calculation with no vertical pattern in g_s and a constant C_i/C_a resulted in $\sim 16\%$ lower A_{nC} , an underestimation found in other single-layer models (DePury & Farquhar, 1997; Lai *et al.*, 2000; Friend, 2001). Thus, the complexity added by using a multilayered model with variable c_i/c_a and g_{CO_2} was necessary to attain closure of the C balance under CO_2^b conditions, and the good agreement between A_{nC} and GPP (Fig. 4b) suggests that the

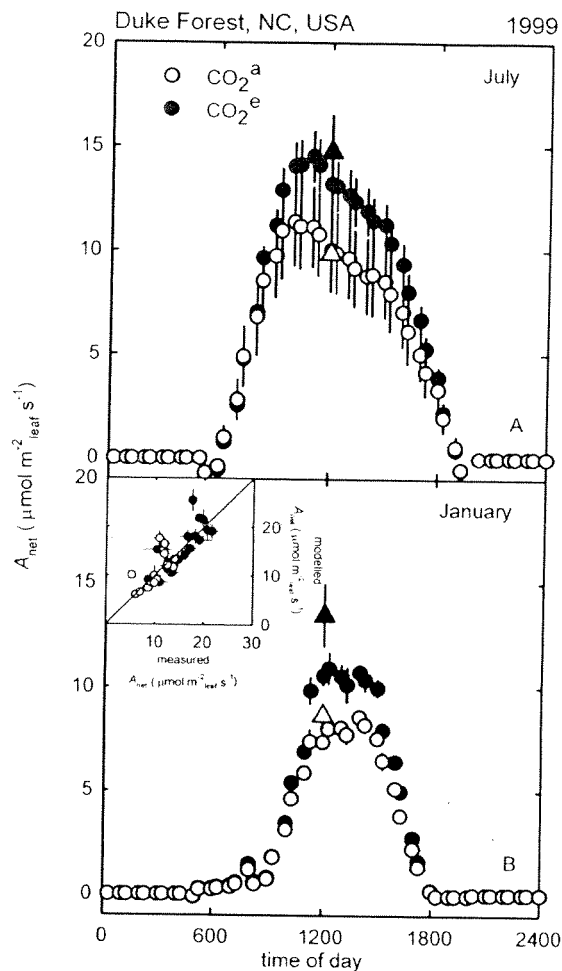


Fig. 5 Comparison of ensemble mean canopy net assimilation (A_{net}) for the upper canopy third (corresponding to mostly sunlit leaves) with midday measurements of A_{net} via leaf gas exchange measurements (shown as triangles) for a warm (July) and a cold (January) month in 1999 ($n = 3$ treatment plots; bars represent 1 standard error). The inset shows upper canopy midday modelled A_{net} vs. midday A_{net} measured via leaf gas exchange measurements for both months with the 1:1 line for reference.

estimate based on the sum of flux components is a little low.

As a final test of our multilayered model, we compared A_{net} estimates of sun foliage in the upper *P. taeda* canopy with gas exchange measured midday values (Ellsworth, 2000). The diurnal A_{net} pattern in the upper one-third of the canopy obtained through a monthly ensemble average of estimates from the 4C-A model is shown along with the leaf gas exchange measured values for a midsummer and a midwinter month, with favourable and unfavourable conditions for photosynthesis, respectively (Fig. 5). This analysis was repeated throughout the year for every month in

which leaf gas exchange measurements were available, showing a good agreement between the 4C-A and leaf gas exchange values (inset in Fig. 5: each datum represents a different month); the few points clearly above unity reflect a higher stomatal conductance calculated for the whole canopy relative to that measured with leaf gas exchange measurements on a small section of fascicles. In (Fig. 5), we also show the only test available of the model performance under CO₂^e, demonstrating that the model is able to reproduce direct measurements of A_{net} under CO₂^e. Schäfer *et al.* (2002) observed that the elevated CO₂ did not affect transpiration at the stand. Using their transpiration data and the 4C-A estimate of A_{nC} , stand level water use efficiency was 4.7 g C kg⁻¹ H₂O under CO₂^a and 7.0 g C kg⁻¹ H₂O under CO₂^e, similar to leaf-level values for the *P. taeda* at this stand (Ellsworth, 1999).

Effects of elevated CO₂

The seasonal pattern of monthly A_{nC} and associated R_C , R_M and F_C^f under CO₂^e is shown in (Fig. 3b–e). The pattern is similar, although not identical to that under CO₂^a, but with greater amplitude. A_{nC} on a monthly basis under CO₂^e was linearly correlated with that under CO₂^a, for both *P. taeda* (slope 1.34) and the broadleaf species (slope 1.67), and for the entire canopy (slope 1.41, minimum $r^2 = 0.98$; $P < 0.0001$).

The effect of CO₂^e on modelled A_{nC} (expressed as A_{nC} under CO₂^e divided by that under CO₂^a) was slightly greater for *P. taeda* in 2000 than in 1999, with the opposite occurring for the broadleaf species. However, the difference between years was not significant ($P > 0.35$) and the response in both years was averaged for presentation (Fig. 6). Modelled A_{nC} was 34% higher in CO₂^e plots in *P. taeda* and 67% higher in broadleaf species than in CO₂^a plots (see overall effect, Fig. 6). Several factors can contribute to the enhancement of modelled A_{nC} based on the 4C-A model: (1) elevated atmospheric CO₂ concentration; (2) effect of CO₂^e on stomatal conductance; (3) effect of CO₂^e on CE_{max} ; and (4) effect of CO₂^e on L and, in the Duke Forest FACE, pretreatment differences in L even though plots were paired prior to the onset of enrichment to minimized differences. The contribution of each factor to the overall effect was evaluated by running the model with only one factor at a time representing the conditions of the plots under CO₂^e. Our results show that the potential enhancement solely due to CO₂^e is ~55% for both species types (Fig. 6). Higher *P. taeda* stomatal conductance due to increased water availability in CO₂^e plots could potentially increase A_{nC} under otherwise CO₂^a conditions by 5%. The broadleaf species showed a reduction of 3% in A_{nC} due to

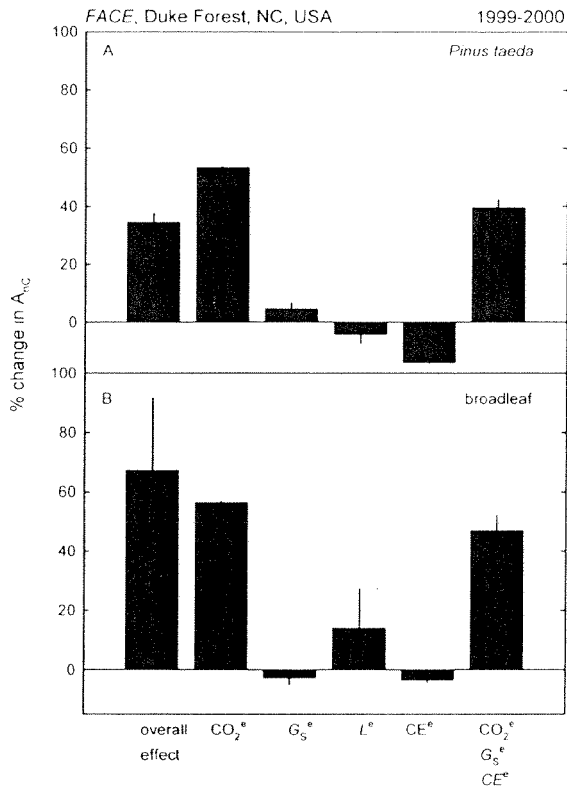


Fig. 6 Effect of different components on canopy net assimilation (A_{nC}) for *P. taeda* (a) and the broadleaf canopy (b) as a % change of effect vs. ambient conditions (see text). First a comparison was made between elevated and ambient plots with the model parameterized best to represent each set of plots ('overall effect'). Then, components were altered in ambient plots to represent differences in a single parameter, or a combination of parameters, with elevated CO_2 plots. The resulting model runs altered the CO_2 concentration itself (CO_2^*), canopy stomatal conductance (G_s^*), leaf area index (L^*), carboxylation efficiency (CE^*), and a combination of all but L^* .

stomatal response to CO_2 . Leaf area index did not respond to CO_2 in this experiment; thus, using L from CO_2^* plots to estimate A_{nC} under otherwise CO_2^* conditions reflects mostly differences in initial conditions in which L of *P. taeda* was slightly lower under CO_2^* and that of the broadleaf was slightly higher. For both species the potential change in A_{nC} due to the inherent initial difference in L was not significant ($P > 0.29$), but influenced the overall effect. Down-regulation of CE_{max} by different needle age classes reduced A_{nC} of *P. taeda* by 14% and that of the broadleaf species by 4%. Thus, we estimated A_{nC} exclusive of inherent, pretreatment differences among plots by using the values of L found for different species in the CO_2^* plots with all other factors as in the CO_2^* plots. The estimated CO_2 effect in this forest is 39% and 47% for *P.*

taeda and the broadleaf species, respectively, or 41% for the entire canopy.

Based on paired *t*-test comparisons of NPP and respiration estimates between treatments, only R_C and NPP for *P. taeda* and the entire stand in 1999 showed a significant difference between treatments (Table 3). We average the components of the autotrophic C balance for the two years (shown in Table 3) and present them together with the additional ecosystem C balance components to facilitate a comparison between treatments (Table 4). The major components of the autotrophic and whole ecosystem C balance (taken from Table 4) are presented in Fig. 7. We also calculated certain ratios amongst C balance components (Table 5) to compare under ambient conditions with commonly published ratios, and under elevated CO_2 conditions with ratios available from studies using different approaches at this site.

Monthly estimates of A_{nC} were related to stand level transpiration (E_C ; Schäfer *et al.* 2002). A_{nC} was linearly related to E_C under both CO_2^* and CO_2^* (minimum $r^2 = 0.87$; $P < 0.0001$) without observable differences among years (minimum $P = 0.14$), and with 50% higher water use efficiency under CO_2^* ($P < 0.0001$). This enhancement in water use efficiency is greater than the 13% calculated based on GPP due to the 20% lack of closure in the C balance under CO_2^* , as opposed to the closure obtained under CO_2^* (Table 4; Fig. 7).

Discussion

During the third and fourth years of this experiment, the uptake of CO_2 by the plant canopy under CO_2^* was significantly greater ($1010 \text{ g C m}^{-2} \text{ a}^{-1}$ or 41% enhancement) than under CO_2^* (Figs 2 and 3; Table 3). The additional C that was assimilated under CO_2^* was allocated to tree growth ($243 \text{ g C m}^{-2} \text{ a}^{-1}$ during the 1999 and 2000 growing seasons) and respiration ($129 \text{ g C m}^{-2} \text{ a}^{-1}$). Most of the remaining extra C is unaccounted for by the measured or modelled fluxes of C in this study (Table 4; Fig. 7). The lack of closure in our C budgets under CO_2^* is in sharp contrast to the near-complete closure under CO_2^* . This, coupled with the observation that modelled gas exchange agreed with measured leaf-level values equally well under both CO_2 conditions (Fig. 5), suggests that one or more C budget components is underestimated following fixation under CO_2^* . In what follows, we analyse and discuss the pools and fluxes that may account for this 'missing' C.

Assessment of C balance under ambient CO_2

Estimating CO_2 uptake using process-based ('bottom-up') or empirical ('top-down') approaches has been an

Table 4 Plant and ecosystem components in g C m⁻² a⁻¹ averaged for 1999 and 2000

Scale	CO ₂	CO ₂
<i>Daytime ecosystem C balance</i>		
<i>A</i> _{nc}	2449	
<i>F</i> _c ^g	-1175	
<i>F</i> _c ^g daytime	-540	
<i>ΔS</i> _c ^a	-22	
<i>R</i> _{MA} daytime	-280	
<i>R</i> _{CA} daytime	-116	
LOC	316	
<i>Plant C balance</i>		
<i>A</i> _{nc}	2449	3459
GPP	2396	2759
<i>R</i> _A	1402	1531
<i>R</i> _M	1155	1233
<i>R</i> _{MA}	532	561
<i>R</i> _{MB}	623	672
<i>R</i> _C	246	298
<i>R</i> _{CA}	230	278
<i>R</i> _{CB}	16	20
NPP	994	1228
growth	750	960
Alitter	222	241
Aroots	14	20
DOC	8	7
LOC	53	700
<i>Heterotrophic C balance</i>		
<i>R</i> _H	407	930
<i>F</i> _c ^g	1046	1621
<i>R</i> _{AB} *	639	691
INPUT	342	404
litter	320	377
DOC	8	7
root turnover	14	20
Astorage	-15	80
Aforest floor	42	50
Aroot	4	6
Asoil C	-61	24
Input - Astorage	357	324
LOC	50	606
<i>Ecosystem (24 h)</i>		
NEE	721	
NEP Ia	585	301
NPP	986	1221
<i>R</i> _{Hg} I	407	930
<i>R</i> _H I	7	10
LOC I	136	
NEP Ib	636	907
NPP	986	1221
<i>R</i> _{Hg} II	357	324
<i>R</i> _H II	7	10
LOC II	91	
NEP II	613	885
ΔB _s	633	811
Aforest floor	42	50
Asoil C	-61	24
LOC III	114	

*DIC is not considered. DIC was 16 g C m⁻² a⁻¹ under CO₂ and 22 g C m⁻² a⁻¹ under CO₂; subscript g and I in the *Ecosystem R*_H component refers to CO₂ losses in gas and liquid form, respectively.

active field of research for more than four decades (Duncan *et al.*, 1967; Monteith, 1977, see Jarvis *et al.*, 1985). Balancing the C budget to account for *A*_{nc} by independent measurements of biomass production and estimates of respiration of individual branches, trees, and canopies builds confidence in the skills of models to estimate *A*_{nc} and respiration. These skills are especially important when productivity might not be accurately measured, as is often the case in below-ground measurements, and is estimated as the residual of the C balance between *A*_{nc} and the sum of respiration and above-ground productivity (Schulze *et al.*, 1977; Matyssek & Schuize, 1988; Oren & Zimmermann, 1989; Law *et al.*, 2000). Recently, C balances have been cross-validated by comparing modelled *A*_{nc} with ecosystem scale CO₂ fluxes measured with eddy covariance, or with NPP and plant respiration (Wofsy *et al.*, 1993; Baldocchi *et al.* 1996, Arneeth *et al.* 1998, Granier *et al.* 2000, Lai *et al.* 2002). When modelled fluxes of C are in simultaneous agreement with independently measured fluxes of C from both plant and ecosystem pools, it is possible to conclude that the modelled estimate of *A*_{nc} has a high degree of accuracy. We are aware of only a few studies that have utilized such an approach (e.g. Granier *et al.*, 2000; Law *et al.*, 2000).

In this study, monthly *A*_{nc} under CO₂ was higher (~13%) than estimated based on eddy covariance measurements (Fig. 4a), but very similar to (within 3% of) the annual GPP estimate based on growth and respiration (Fig. 4b). The discrepancy with the estimate based on eddy covariance is within the spatial variability in fluxes measured over this stand (Katul *et al.*, 1999). The 4C-A estimate of *A*_{nc} under CO₂ is twice that estimated with MAESTRA (Luo *et al.*, 2001) and one-third higher than that estimated with a light response curve and a constrained source-optimization model that neglects above-ground daytime respiration (CSO; Lai *et al.*, 2002; Table 6). Our estimate of GPP in 1999 and 2000 is ~100 g m⁻² a⁻¹ greater and smaller, respectively, than the estimate of GPP presented by Hamilton *et al.* (2002) for the 1998 calendar year. The difference between our study and that of Hamilton *et al.* (2002) reflects methodological differences (e.g. Hamilton *et al.* (2002) include daytime photorespiration, which is not included in our model), and annual variation in growing conditions superimposed on the dynamics of this rapidly aggrading forest ecosystem.

In addition to working at the stand level, we compared the modelled estimates of *A*_{nc} with NPP plus autotrophic construction and maintenance respiration (= GPP) for *P. taeda* and the broadleaf species separately. Averaged over 1999 and 2000, the *A*_{nc} of the broadleaf component was 20% higher than that present-

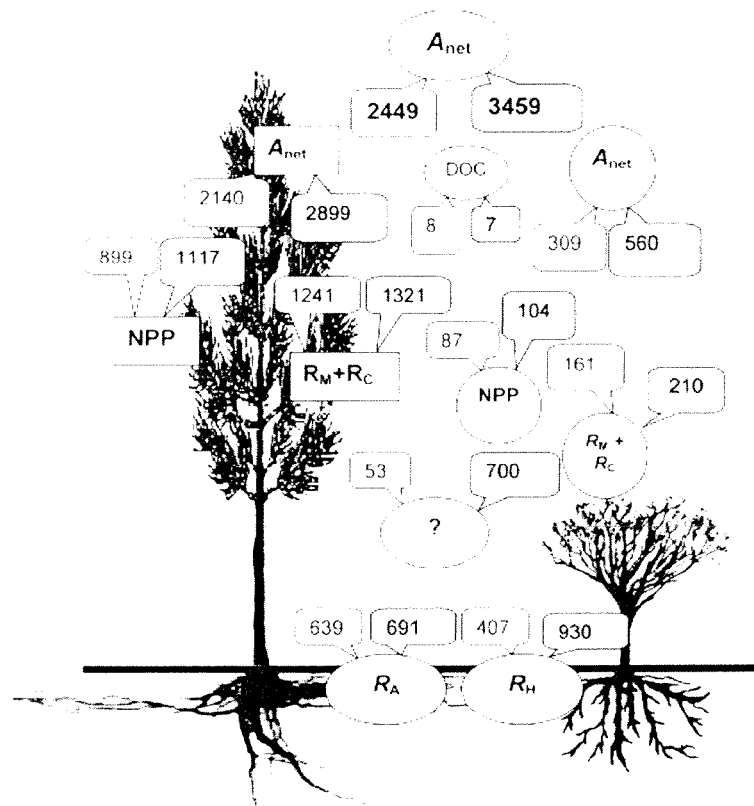


Fig. 7 Components of the forest carbon balance averaged for 1999 and 2000. Components identified in ellipsoid boxes are for the entire ecosystem, in squares are for *Pinus taeda* (terms on the left-hand side), and in circles are for the broadleaf canopy (terms on the right-hand side). Shown are canopy net assimilation, a_{nC} , net primary productivity, NPP , construction respiration, R_C , combined with maintenance respiration, R_M , and the amount of CO_2 efflux from the forest floor attributed to autotrophic and heterotrophic respiration, R_A and R_H , respectively. The lack of closure in the autotrophic carbon balance is shown as '?'.

ted in Hamilton *et al.* (2002) (Fig. 7). In contrast, there was very strong agreement between studies in GPP for the *P. taeda* component of this ecosystem (Table 3).

We evaluated our C balance under ambient conditions by comparing commonly calculated ratios between balance components (Table 5) with published values. Our NPP/GPP ratio was slightly lower (Table 5) than a general ratio estimated for a large number of stands (0.47) by Landsberg & Waring (1997). Our R_A/GPP ratio ($= 1 - NPP/GPP$, similar to R_A/A_{nC}) is within the range calculated based on the amount of standing biomass or tree height (Ryan *et al.*, 1994; Mäkelä & Valentine, 2001; Table 5), higher than the 0.42 estimated for 1999 by Lai *et al.* (2002) and lower than the 0.7 estimated for 1998 by Hamilton *et al.* (2002). Notably, Hamilton *et al.* (2002) include estimates of daytime foliage respiration in their estimate while Lai *et al.* (2002) neglected daytime above-ground respiration.

The F_C^H/NPP ratio was lower in this study than the 'global' average ratio of 1.24 (Raich & Schlesinger 1992) and the 1.65 estimated in a young *Pinus ponderosa* L.

stand (Law *et al.*, 1999). It is likely that our stand is at a different stage of development in which much of the assimilated C is invested in slow turnover woody biomass. Subtracting R_A (both construction and maintenance) of roots from total F_C^H (Table 4), we estimated that $\sim 38\%$ ($407 \text{ g C m}^{-2} \text{ a}^{-1}$) of this flux was due to heterotrophic respiration. This proportion is in agreement with values obtained with a similar methodology in similar stands (Maier & Kress 2000), but lower than the 45% that was estimated by Andrews *et al.* (1999) in the plots under CO_2^s using isotopic mixing ratios. This may reflect lower rates of rhizodeposition under CO_2^s (Table 4). R_H estimated by Hamilton *et al.* (2002) as the difference between F_C^H and R_A was 22% of F_C^H (Table 6), allowing only $216 \text{ g C m}^{-2} \text{ a}^{-1}$ on average to balance C turnover in the forest floor–soil subsystem – significantly lower than the estimate in this study. Assuming, as a lower boundary, that the forest floor C is at steady state under CO_2^a , the sum of C in (1) litterfall (Finzi *et al.* 2001, 2002), (2) the turnover of fine roots (Matamala & Schlesinger, 2000), (3) dissolved in organic forms in

Table 5 Ratios of respiration components (autotrophic R_A , heterotrophic R_H , construction R_C , maintenance R_M and soil CO₂ efflux F_C^H) under ambient (CO₂) and elevated (CO₂^e) atmospheric CO₂ concentrations with gross primary productivity (GPP) and modelled canopy net assimilation (A_{nC}). Bold type indicates differences significant at $P \leq 0.009$

Ratio	CO ₂	CO ₂ ^e	<i>P</i> value
R_A/A_{nC}	0.58 (0.028)	0.44 (0.027)	0.03
R_A/GPP	0.58 (0.012)	0.55 (0.009)	0.05
	0.55–0.60*		
	0.57–0.59†		
R_C/A_{nC}	0.10 (0.004)	0.09 (0.004)	0.01
R_C/GPP	0.10 (0.004)	0.10 (0.003)	0.22
R_M/A_{nC}	0.48 (0.028)	0.36 (0.024)	0.04
R_M/GPP	0.48 (0.016)	0.44 (0.012)	0.07
R_H/F_C^H	0.38 (0.090)	0.57 (0.050)	0.13
F_C^H/NPP	1.07 (0.060)	1.36 (0.084)	< 0.01

R_H was calculated as the difference between F_C^H and root respiration (construction and maintenance). All ratios are averages for 1999 and 2000.

Mean of 2 years and three plots and 1 standard error from the mean in parentheses.

*Based on Mäkelä & Valentine (2001).

†Generated after equation $R_A/GPP = 0.6191 (1 - e^{0.00048S})$ derived from Ryan *et al.* (1994).

precipitation (DOC), (4) and depleted from the mineral soil (1.43–1.31% over 3 years; see Schlesinger & Lichter, 2001) would release $357 \text{ g C m}^{-2} \text{ a}^{-1}$ (cf. Table 4). This C release accounts for 88% of our estimate of R_H , leaving us with the need to account for $\sim 50 \text{ g m}^{-2} \text{ a}^{-1}$. Richter *et al.* (1999) estimated that root exudation in young *P. taeda* stands is $\sim 50 \text{ g m}^{-2} \text{ a}^{-1}$ and can account for the remaining flux of C from the top of the forest floor (Table 3, 4; Fig. 7).

In summary, the budget for C in autotrophic and whole-ecosystem components is balanced under CO₂. The pools and fluxes of the measured components are reasonable in absolute terms, relative to each other, and are similar to values published in the literature. Based on this, we applied the same set of analyses to the balances of C in the forest plots under CO₂^e.

Assessment of C balance under elevated CO₂

Applying the 4C-A model to CO₂^e conditions produced an enhancement of A_{nC} by 41% relative to that under CO₂ (a 35% and 67% stimulation for the *P. taeda* and broadleaf components, respectively; Fig. 6). This enhancement is reduced to 39% when we factor out the pre treatment difference in leaf area index (L) between the plots under CO₂^e and CO₂. Both enhancement ratios are similar to that modelled for the 1998 calendar year

(43%) by Luo *et al.* (2001). The 4C-A model estimated an enhancement of 55% in A_{nC} due to elevated CO₂, and in addition a 5% enhancement due to increase in G_S of *P. taeda* (Fig. 6). Canopy stomatal conductance of *P. taeda* increased with increasing water availability under CO₂^e (Schäfer *et al.*, 2002, in review). The model also estimated a decline of 3% in A_{nC} due to a decrease in G_S of the broadleaf species, and 14% due to a progressive decline in CE_{max} , mostly in previous-year foliage of *P. taeda* (Rogers & Ellsworth, 2002) that assimilates 70% of annual A_{nC} (Fig. 6). In absolute terms, the enhancement in A_{nC} attributable to the effect of CO₂^e was $963 \text{ g C m}^{-2} \text{ a}^{-1}$. This value is lower than the $1010 \text{ g C m}^{-2} \text{ a}^{-1}$ value (Fig. 7), reflecting the effect of pretreatment differences in L (Fig. 6).

GPP – based on production and respiration – was only enhanced by 13% under CO₂^e. This enhancement is lower than the 18% that was estimated for the 1998 calendar year (Hamilton *et al.* 2002), and less than half that estimated for A_{nC} by the 4C-A model. The enhancement in GPP is attributable to a 23% increase in NPP , a slight reduction over that observed in the second year of CO₂ enrichment (26%, DeLucia *et al.*, 1999; Hamilton *et al.*, 2002). Averaging across years, *P. taeda* wood production was enhanced by 29% under CO₂^e and broadleaf wood production by 34% (Table 3). This resulted in a 29% enhancement of C storage in woody biomass, a moderately long-term storage pool of C. The other component of GPP , autotrophic respiration (R_A), was enhanced by 13% under CO₂^e, in contrast to Hamilton *et al.* (2002) who reported a 6% decline in this flux. Their reduction in R_A was due to a decrease in the rate of root R_M under CO₂^e. Estimates of specific respiration rates obtained from excised and intact roots are subject to methodological artefact (Clinton & Vose, 1999; McDowell *et al.*, 1999; Matamala & Schlesinger, 2000). The reduction in R_M reported by Hamilton *et al.* (2002) contrasts with the increase reported by Matamala & Schlesinger (2000) for this FACE site and on which we based our calculations.

In contrast to the similarity in F_C^H under CO₂^e, we estimated much higher F_C^H under CO₂^e than did Hamilton *et al.* (2002) at 602 and $248 \text{ g C m}^{-2} \text{ a}^{-1}$, respectively. The 54% enhancement under CO₂^e is well within the range of reported values from the prototype FACE plot at this site (Andrews *et al.*, 1999). It is also similar to that found for *P. ponderosa* under CO₂^e (Johnson *et al.*, 1994). At the Duke Forest FACE site, the CO₂ enhancement in mean annual midday F_C^H increased from 24% in 1997 to 43% in 1998 (Andrews *et al.*, 1999), suggesting that F_C^H was still responding to the step increase in atmospheric CO₂ commencing in August 1996.

In this study, R_A contributed $691 \text{ g C m}^{-2} \text{ a}^{-1}$ to F_C^H under CO₂^e, leaving $930 \text{ g C m}^{-2} \text{ a}^{-1}$ for R_H (Table 4).

Table 6 Comparison of estimates of different components of C balance

g C m ⁻² a ⁻¹		DeLucia <i>et al.</i> (1999)		Luo <i>et al.</i> (2001)		Lai <i>et al.</i> (2002)		Hamilton <i>et al.</i> (2002)		This study	
		CO ₂ ^a	CO ₂ ^c	CO ₂ ^b	CO ₂ ^e	CO ₂ ^d	CO ₂ ^a	CO ₂ ^c	CO ₂ ^b	CO ₂ ^e	CO ₂ ^d
GPP	1997			1224	1695						
	1998			1250	1786						
	1999					1808				2287	2622
	2000							2371	2805	2486	2879
NPP	1997	633	744								
	1998							705	897		
	1999									909	1127
	2000									1060	1313
NEP	1997										
	1998							428	602		
	1999					605				576	872
	2000									654	1030
R _e	1997										
	1998										
	1999							1932			
	2000					1203					
R _A	1997										
	1998							1704	1604		
	1999					214				1378	1495
	2000									1426	1567
R _H	1997										
	1998							216	574		
	1999									464	753
	2000									457	749
F _C ^{ff}	1997										
	1998							928	1176		
	1999					989				1051	1620
	2000									1039	1619

Mass balance calculations – assuming that the efflux of C from the forest floor is in a short-term steady state – imply the addition of C to the soil from an unmeasured source. The data presented in Schlesinger & Lichter (2001) suggest that the pool of C in the forest floor and mineral soil horizons under CO₂ is increasing by 80 g C m⁻² a⁻¹. The components that turn over annually – above-ground litterfall, root mortality, and DOC – contribute an additional 404 g C m⁻² a⁻¹ to the forest floor (Table 4). Thus, the difference between R_H plus the increment of C in soil pools (1010 g C m⁻² a⁻¹) and inputs *via* turnover components (404 g C m⁻² a⁻¹) implies a source for C of 606 g C m⁻² a⁻¹ (Fig. 7). This quantity is in very close agreement with the 700 g C m⁻² a⁻¹ of A_{nC} predicted by the 4C-A model and not accounted for by the estimate of GPP from NPP and R_A under CO₂. Rhizodeposition can account for 20% of net CO₂ assimilation, most of which is immediately respired by microbes (Merbach *et al.*, 1999). Thus, the higher R_H/F_C^{ff} obtained under CO₂ than under CO₂

(Table 5) reflects the allocation of C to rhizodeposition and subsequent metabolism by the microbial community (Table 4). The remaining C (700 – 606 = 94 g C m⁻² a⁻¹) is 3% of A_{nC}. This remainder may be explained by measurement error. Alternatively, it may reflect an increase in the allocation of C to fine root and mycorrhizal production in response to increasing nutrient limitation under CO₂ (Norby *et al.*, 1992; Zak *et al.*, 2000; Finzi *et al.*, 2001; Oren *et al.*, 2001; Constable *et al.*, 2001).

Effects of elevated CO₂ on C sequestration

Hamilton *et al.* (2002) estimated that NEP in 1998 (measured as the difference between NPP and R_H) was lower under CO₂ than under CO₂, and we found the same pattern in this study for 1999 and 2000 (Tables 3 and 4, NEP la). The 94 g C m⁻² a⁻¹ modelled by A_{nC}, but unaccounted for by the component C balance method under CO₂, may represent an underestimate of

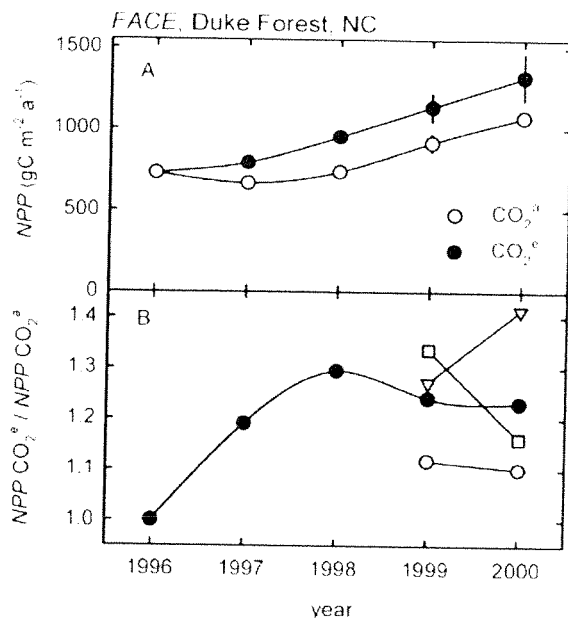


Fig. 8 (a) Net primary productivity (*NPP*) for the first 5 years of CO₂ fumigation in the Duke FACE experiment since commencement in 1996. Data from 1996 and 1997 are taken from DeLucia *et al.* (1999) and in 1998 from Hamilton *et al.* (2002) scaled to the plots in this study (see Discussion). CO₂^e denotes elevated and CO₂^a denotes ambient CO₂ conditions. (b) Enhancement ratio of *NPP* under CO₂^e relative to that under CO₂^a since commencement of fumigation in 1996. The temporal and spatial variation in the response to CO₂^e within each plot pair is shown for 1999 and 2000 (grey symbols, different symbol types represent different plots).

NPP of approximately 7%. Adding this quantity to *NPP* would not make *NEP* Ia under CO₂^e higher than under CO₂^a. To minimize error, we also estimated *NEP* based on two additional methods: *NEP* Ib that relied on estimates of heterotrophic respiration from changes in C pools, but was otherwise calculated as *NEP* Ia (see Table 4), and *NEP* II calculated as the difference between C pools at the end of successive years (Tables 3 and 4, *NEP* II). Both approaches estimated values of *NEP* that were much closer to *NEE* under CO₂^e, providing us with confidence in our estimate. Furthermore, *NEP* calculated based on both approaches was ~270 g C m⁻² a⁻¹ higher under CO₂^e. This additional C is partitioned into the following pools: 235 g C m⁻² a⁻¹ are sequestered in woody biomass and 36 g C m⁻² a⁻¹ are sequestered in soils. The remainder of the extra C taken up by photosynthesis is used in fast turnover pools (e.g. root exudates) at the forest floor–soil subsystem.

We note that not all enhancements in C cycle components were significantly higher under CO₂^e either for *P. taeda*, the broadleaf component, or the stand as a

whole. Notably, there was a large variation in component fluxes in 2000, leading to few statistically significant differences between treatments (Table 3). The reason for the increase in variation is clear when evaluating *NPP* (Table 3; Fig. 8). During the first 2 years of CO₂ fumigation, there was a linear increase in the rate of *NPP* under CO₂^e relative to CO₂^a (Fig. 8b). However, in 1999 and 2000, the ratio remained relatively constant. While the variation in *NPP* under CO₂^a is relatively small, the variation under CO₂^e increased through time (note the size of the standard error bars in Fig. 8a). The variability increased because of increasing differences in CO₂ response of *NPP* among the plot pairs, including a drastic increase in the enhancement ratio of *NPP* for one pair from 1999 to 2000 and a decrease for another (Fig. 8b). Although speculative, the drastic decrease in one of the pairs in the fourth full year of enrichment resembles that observed at the FACE prototype where the decrease was shown to reflect a decline in nutrient availability (Oren *et al.*, 2001).

Conclusion

A combination of methods has demonstrated that the concentration of atmospheric CO₂ predicted for 2060 may increase the rate of C sequestration in woody biomass and soil. These pools represent moderate- to long-term storage of C in the terrestrial biosphere. However, the variation in the response of *NPP* among plots and years indicates that C storage is sensitive to other growth-limiting factors. Soil nutrient availability is a key candidate for this limitation (Eamus & Jarvis, 1989; Körner, 1995), as suggested by the results from a nutrient amendment study at the prototype FACE plot at this site (Oren *et al.*, 2001). If nutrient limitation imposes a constraint on future productivity, it is likely that C allocation to the production of wood will decrease in favour of the allocation to fine root production, rhizodeposition, and mycorrhizal symbionts (Norby *et al.*, 1992, 2001). Allocation of C to these pools will likely result in a rapid return of fixed C to the atmosphere (Merbach *et al.*, 1999). Thus, if nutrient limitations to growth increase at this site (Finzi *et al.*, 2001, 2002), it is possible that high rates of C fixation under elevated CO₂ will result in an acceleration of the C cycle through the forest ecosystem with little of the C remaining in long-term storage pools.

Acknowledgements

The senior author would like to thank J.M. Rivin for insightful discussions and the creation of Fig. 7 and M. Hempel for financial support. The authors would like to thank Y. Para-

shenkov for data assistance, J. Nagy, K. Lewin and G. Hendrey for operating the FACTS-1 site. This study was supported by the US Department of Energy (DOE) through both the Office of Biological and Environmental Research and the National Institute of Global Environmental Change (NIGEC) Southeastern Regional Center at the University of Alabama. This work contributes to the Global Change and Terrestrial Ecosystem (GCTE) core project of the International Geosphere-Biosphere Program (IGBP).

References

- Andrews JA, Harrison KG, Matamala R, Schlesinger WH (1999) Separation of root respiration from total soil respiration using carbon-13 labelling during free-air carbon dioxide enrichment (FACE). *Soil Science Society of America Journal*, **63**, 1429–1435.
- Arneth A, Kelliher FM, McSeveny, Byers JN (1998) Assessment of annual carbon exchange in a water stressed *Pinus radiata* plantation: an analysis based on eddy covariance measurements and an integrated biophysical model. *Global Change Biology*, **5**, 531–545.
- Baldocchi D, Valentini R, Running S, Oechel W, Dahlman R (1996) Strategies for measuring and modelling carbon dioxide and water vapor fluxes over terrestrial ecosystems. *Global Change Biology*, **2**, 159–168.
- Baldocchi D, Meyers T (1998) On using micrometeorological and biophysical theory to evaluate carbon dioxide, water vapor and trace gas fluxes over vegetation: a perspective. *Agriculture and Forest Meteorology*, **90**, 1–25.
- Butnor JR, Johnsen KH, Oren R, Katul GG (2003) Reduction of forest floor respiration by fertilization on both carbon dioxide enriched and reference 17-year-old loblolly pine stands. *Global Change Biology*, **9**, 849–861.
- Campbell GS, Norman JM (1998) *An introduction to environmental biophysics*. 2nd edn. Springer Verlag, New York.
- Carey EV, DeLucia EH, Ball JT (1996) Stem maintenance and construction respiration in *Pinus ponderosa* grown in different concentration of atmospheric CO₂. *Tree Physiology*, **16**, 125–130.
- Clinton BD, Vose JM (1999) Fine root respiration in mature eastern white pine (*Pinus strobus*) *in situ*: the importance of CO₂ controlled environments. *Tree Physiology*, **19**, 475–479.
- Collatz GJ, Ball JT, Grivet C, Berry JA (1991) Physiological and environmental regulation of stomatal conductance, photosynthesis and transpiration: a model that includes a laminar boundary layer. *Agricultural and Forest Meteorology*, **54**, 107–136.
- Constable JVH, Bassirirad H, Lussenhop J, Zerihun A (2001) Influence of elevated CO₂ and mycorrhizae on nitrogen acquisition: contrasting responses in *Pinus taeda* and *Liquidambar styraciflua*. *Tree Physiology*, **21**, 83–91.
- DeLucia E, Hamilton JG, Naidu SL *et al.* (1999) Net primary production of a forest ecosystem with experimental CO₂ enrichment. *Science*, **284**, 1177–1179.
- DeLucia EH, George K, Hamilton JG (2002) Radiation-use efficiency of a forest exposed to elevated concentrations of atmospheric carbon dioxide. *Tree Physiology*, **22**, 1003–1010.
- DePury DGG, Farquhar GD (1997) Simple scaling of photosynthesis from leaves to canopies without the errors of big-leaf models. *Plant, Cell and Environment*, **20**, 537–557.
- Duncan WO, Loomis RS, Williams WA, Hanau R (1967) A model for simulating photosynthesis in plant communities. *Hilgardia*, **38**, 181–203.
- Eamus D, Jarvis PG (1989) The direct effect of increase in the global atmospheric CO₂ concentration on natural and commercial trees and forests. *Advances in Ecological Research*, **19**, 1–55.
- Ellsworth DS (1999) CO₂ enrichment in a maturing pine forest: are CO₂ exchange and water status in the canopy affected? *Plant, Cell and Environment*, **22**, 461–472.
- Ellsworth DS (2000) Seasonal CO₂ assimilation and stomatal limitations in a *Pinus taeda* canopy with varying climate. *Tree Physiology*, **20**, 435–445.
- Erbs DG, Klein SA, Duffie JA (1982) Estimation of the diffuse radiation fraction for hourly, daily and monthly average global radiation. *Solar Energy*, **28**, 293.
- Ewers BE, Oren R (2000) Analysis of assumptions and errors in the calculation of stomatal conductance from sap flux measurements. *Tree Physiology*, **20**, 579–589.
- Farquhar GD, von Caemmere S, Berry JA (1980) A biochemical model of photosynthetic CO₂ assimilation in leaves of C3 species. *Planta*, **149**, 78–90.
- Finzi AC, Alien AS, DeLucia EH, Ellsworth DS, Schlesinger WH (2001) Forest litter production, chemistry and decomposition following two years of free-air CO₂ enrichment. *Ecology*, **82**, 470–484.
- Finzi AC, DeLucia EH, Hamilton JG, Richter DD, Schlesinger WH (2002) The nitrogen budget of a pine forest under elevated CO₂ enrichment. *Oecologia*, **132**, 567–578.
- Friend AD (2001) Modelling canopy CO₂ flux: are 'big-leaf' simplifications justified? *Global Ecology & Biogeography*, **10**, 603–619.
- Granier A (1987) Evaluation of transpiration in a Douglas-fir stand by means of sap flow measurements. *Tree Physiology*, **3**, 309–320.
- Granier A, Ceschia E, Damesin C *et al.* (2000) The carbon balance of a young Beech forest. *Functional Ecology*, **14**, 312–325.
- Griffin KL, Thomas RB, Strain BR (1993) Effects of nitrogen supply and elevated carbon dioxide on construction cost in leaves of *Pinus taeda* L. seedlings. *Oecologia*, **95**, 575–580.
- Griffin KL, Tissue DT, Turnbull MH, Whitehead D (2001) The onset of photosynthetic acclimation to elevated CO₂ partial pressure in field-grown *Pinus radiata* D. Don after 4 years. *Plant, Cell and Environment*, **23**, 1089–1098.
- Griffin KL, Winner WE, Strain BR (1996) Construction cost of loblolly and ponderosa pine leaves grown with varying carbon and nitrogen availability. *Plant, Cell and Environment*, **19**, 729–738.
- Hamilton JG, DeLucia EH, George K, Naidu SL, Finzi AC, Schlesinger WH (2002) Forest carbon balance under elevated CO₂. *Oecologia*, **131**, 250–260.
- Hamilton JG, Thomas RB, DeLucia EH (2001) Direct and indirect effects of elevated CO₂ on leaf respiration in a forest ecosystem. *Plant, Cell and Environment*, **24**, 975–982.
- Hendrey GR, Ellsworth DS, Lewin KE, Nagy J (1999) A free-air enrichment system for exposing tall forest vegetation to elevated atmospheric CO₂. *Global Change Biology*, **5**, 293–309.
- Herrick J, Thomas RB (1999) Effects of CO₂ enrichment on the photosynthetic light response of sun and shade leaves of

- canopy sweetgum trees (*Liquidambar styraciflua*) in a forest ecosystem. *Tree Physiology*, **19**, 779–786.
- Herrick J, Thomas RB (2001) No photosynthetic down-regulation in sweetgum trees (*Liquidambar styraciflua* L.) after three years of CO₂ enrichment at the Duke Forest FACE experiment. *Plant, Cell and Environment*, **24**, 53–64.
- Houghton JT (1997) *Global Warming. The Complete Briefing*. Cambridge University Press, Cambridge pp. 251.
- Jach ME, Ceulemans R (2000) Effects of season, needle age and elevated atmospheric CO₂ on photosynthesis in Scots pine (*Pinus sylvestris*). *Tree Physiology*, **20**, 145–157.
- Jarvis PG, Miranda HS, Muetzenfeld RI (1985) Modelling canopy exchange of water vapor and carbon dioxide in coniferous forest plantations. In: *The Forest-Atmosphere Interaction* (eds Hutchison BA & Hicks BB), pp. 521–542. D. Reidal Publishing Company, Dordrecht, The Netherlands.
- Johnson D, Geisinger D, Walker R, Newman J, Vose J, Elliot K, Ball T (1994) Soil pCO₂, soil respiration, and root activity in CO₂-fumigated and nitrogen fertilized ponderosa pine. *Plant and Soil*, **165**, 129–138.
- Katul G, Hsieh CI, Bowling D *et al.* (1999) Spatial variability of turbulent fluxes in the roughness sublayer of an even-aged pine forest. *Boundary Layer Meteorology*, **93**, 1–28.
- Katul GG, Ellsworth DS, Lai C-T (2000) Modelling assimilation and intercellular CO₂ from measured conductance: a synthesis of approaches. *Plant, Cell and Environment*, **23**, 1313–1328.
- Kinerson RS, Higginbotham KO, Chapman RC (1974) The dynamics of foliage distribution within a forest canopy. *Journal of Applied Ecology*, **11**, 347–353.
- Körner C (1995) Towards a better experimental basis for upscaling plant responses to elevated CO₂ and climate warming. *Plant, Cell and Environment*, **18**, 1101–1110.
- Köstner BMM, Schulze E-D, Kelliher FM *et al.* (1992) Transpiration and canopy conductance in a pristine broad leaved forest of *Nothofagus*: an analysis of xylem sap flow and eddy correlation measurements. *Oecologia*, **91**, 350–359.
- Lai C-T, Katul GG, Butnor J, Ellsworth D, Oren R (2002) Modelling night-time ecosystem respiration by a constrained source optimization method. *Global Change Biology*, **8**, 124–141.
- Lai C-T, Katul GG, Oren R, Ellsworth DS, Schäfer KVR (2000) Modeling CO₂ and water vapor turbulent flux distributions within a forest canopy. *Journal of Geophysical Research*, **105**, 26333–26351.
- Landsberg J, Waring R (1997) A generalized model of forest productivity using simplified concepts of radiation-use efficiency, carbon balance and partitioning. *Forest Ecology and Management*, **95**, 209–228.
- Law BE, Ryan MG, Anthoni PM (1999) Seasonal and annual respiration of a ponderosa pine ecosystem. *Global Change Biology*, **5**, 169–182.
- Law BE, Waring RH, Anthoni PM, Aber JD (2000) Measurements of gross and net ecosystem productivity and water vapour exchange of a *Pinus ponderosa* ecosystem, and an evaluation of two generalized models. *Global Change Biology*, **6**, 155–168.
- Leuning R (1995) A critical appraisal of a combined stomatal-photosynthesis model for C3 plants. *Plant, Cell and Environment*, **18**, 339–355.
- Leuning R, Dunin FX, Wang Y-P (1998) A two-leaf model for canopy conductance, photosynthesis and partitioning of available energy. II. Comparison with measurements. *Agricultural and Forest Meteorology*, **91**, 113–125.
- Luo Y, Chen JL, Reynolds JE, Field CB, Mooney HA (1997) Disproportional increase in photosynthesis and plant biomass in a Californian grassland exposed to elevated CO₂: a simulations analysis. *Functional Ecology*, **11**, 696–704.
- Luo Y, Medlyn B, Hui D, Ellsworth D, Reynolds J, Katul G (2001) Gross primary productivity in Duke forest: modelling synthesis of CO₂ experiment and eddy-flux data. *Ecological Applications*, **11**, 239–252.
- Maier CA (2001) Stem growth and respiration in loblolly pine plantation differing in resource variability. *Tree Physiology*, **21**, 1183–1193.
- Maier CA, Kress LW (2000) Soil CO₂ evolution and root respiration in 11 year-old loblolly pine (*Pinus taeda*) plantations as affected by soil moisture and nutrient availability. *Canadian Journal of Forest Research*, **30**, 347–359.
- Maier CA, Zarnoch SJ, Dougherty PM (1998) Effects of temperature and tissue nitrogen on dormant season stem and branch maintenance respiration in a young loblolly pine (*Pinus taeda*) plantation. *Tree Physiology*, **18**, 11–20.
- Mäkaelä A, Valentine HT (2001) The ratio of *NPP*:*GPP*: evidence of change over the course of stand development. *Tree Physiology*, **21**, 1015–1030.
- Matamala R, Schlesinger WH (2000) Effects of elevated CO₂ on fine root production and activity in an intact temperate forest ecosystem. *Global Change Biology*, **6**, 967–980.
- Matussek R, Schuize E-D (1988) Carbon uptake and respiration in above ground parts of *Larix decidua* X *leptopsis* tree. *Trees*, **2**, 233–241.
- McDowell NG, Marshall JD, Qi J, Mattson K (1999) Direct inhibition of maintenance respiration in western hemlock roots exposed to ambient and soil carbon dioxide concentrations. *Tree Physiology*, **19**, 599–605.
- Merbach W, Mirus E, Knof G, Remus R, Ruppel S, Russow R, Gransee A, Schuize J (1999) Release of carbon and nitrogen compounds by plant roots and their possible ecological importance. *Journal of Plant Nutrition and Soil Science – Zeitschrift für Pflanzenernährung und Bodenkunde*, **162**, 373–383.
- Monteith JL (1977) Climate and the efficiency of crop production in Britain. *Philosophical Transactions of the Royal Society of London Series B*, **281**, 277–294.
- Naidu SL, DeLucia EH, Thomas RB (1998) Contrasting pattern of biomass allocation in dominant and suppressed loblolly pine. *Canadian Journal of Forest Research*, **28**, 1116–1124.
- Naumburg ES, Ellsworth DS (2000) Photosynthetic sunfleck utilization potential of understory saplings growing under elevated CO₂ in FACE. *Oecologia*, **122**, 163–174.
- Norby RJ, Gunderson CA, Wullschlegel SD, O'Neill EG, McCracken MK (1992) Productivity and compensatory response of yellow poplar trees in elevated CO₂. *Nature*, **357**, 322–324.
- Norby RJ, Todd DE, Fults J, Johnson DW (2001) Allometric determination of tree growth in CO₂ enriched sweetgum stand. *New Phytologist*, **150**, 477–487.

- Norman JM (1982) Simulation of microclimates. In: *Biometeorology and Integrated Pest Management* (eds Hatfield JL, Thompson D), pp. 65–99. Academic Press, New York.
- Oren R, Zimmermann R (1989) CO₂ assimilation and the carbon balance of healthy and declining Norway spruce stands. In: *Forest Decline and Air Pollution: a Study of Spruce (Picea abies (L.) Karst.) on acid soils*. Ecological Studies Series, Vol. 77 (eds Schulze E-D, Lange OL, Oren R), pp. 352–369. Springer Verlag, Berlin.
- Oren R, Ellsworth DS, Johnson KH *et al.* (2001) Soil fertility limits carbon sequestration by forest ecosystems in a CO₂-enriched atmosphere. *Nature*, **411**, 469–472.
- Oren R, Pataki D (2001) Transpiration in response to variation in microclimate and soil moisture in southeastern deciduous forests. *Oecologia*, **127**, 549–559.
- Pataki D, Oren R, Tissue D (1998) Elevated carbon dioxide does not affect average canopy stomatal conductance of *Pinus taeda* L. *Oecologia*, **117**, 47–52.
- Phillips N, Oren R (2001) Inter- and intra-specific variations in transpiration in a pine forest. *Ecological Applications*, **11**, 385–396.
- Phillips NG, Nagchadhuri A, Oren R, Katul G (1997) Time constant for water uptake in loblolly pine estimated from time-series of stem sap-flow and evaporative demand. *Trees*, **11**, 412–419.
- Raich JW, Schlesinger WH (1992) The global carbon-dioxide flux in soil respiration and its relationship to climate. *Tellus*, **B44**, 81–99.
- Rey A, Jarvis PG (1998) Long-term photosynthetic acclimation to increased atmospheric CO₂ concentration in young birch (*Betula pendula*) trees. *Tree Physiology*, **18**, 441–450.
- Richter DD, Markewitz D, Trumbore SE, Wells CG (1999) Rapid accumulation and turnover of soil carbon in a re-establishing forest. *Nature*, **400**, 56–58.
- Rogers A, Ellsworth DS (2002) Photosynthetic acclimation of *Pinus taeda* (loblolly pine) to long-term growth in elevated pCO₂ (FACE). *Plant, Cell and Environment*, **25**, 851–858.
- Ryan MG, Under S, Vose J, Hubbard RM (1994) Dark respiration in pines. In: *Environmental Constraints on the Structure and Productivity of Pine Forest Ecosystems: a Comparative Analysis*. *Ecological Bulletins*, **43** (eds Gholz HL, Linder S, McMurtie RE), pp. 50–63.
- Schäfer KVR, Oren R, Lai C-T, Katul GG (2002) Hydrologic balance in an intact temperate forest ecosystem under ambient and elevated atmospheric CO₂ concentration. *Global Change Biology*, **8**, 895–911.
- Schäfer KVR, Phillips N, Oren R (in review). Long-term response to CO₂-enriched atmosphere observed in the canopy stomatal conductance of four tree species under naturally varying environment.
- Schimel DS, House JL, Hibbard KA *et al.* (2001) Recent patterns and mechanisms of carbon exchange by terrestrial ecosystems. *Nature*, **414**, 169–172.
- Schlesinger WH, Lichter J (2001) Limited carbon storage in soil and litter of experimental forest plots under increased atmospheric CO₂. *Nature*, **411**, 466–469.
- Schulze E-D, Fuchs MI, Fuchs M (1977) Spatial distribution of photosynthetic capacity and performance in a mountain spruce forest of northern Germany I. Biomass distribution and daily CO₂ uptake in different crown layers. *Oecologia*, **29**, 43–61.
- Steffen W, Noble I, Canadell J, Apps M, Schulze E-D, Jarvis PG (1998) The terrestrial carbon cycle: implications for the Kyoto Protocol. *Science*, **280**, 1393–1394.
- Stenberg P (1998) Implications of shoot structure on the rate of photosynthesis at different levels in a coniferous canopy using a model incorporating grouping and penumbra. *Functional Ecology*, **12**, 82–91.
- Tissue DT, Griffin KL, Turnbull MH, Whitehead D (2001) Canopy position and needle age affect photosynthetic response in field-grown *Pinus radiata* after five years of exposure to elevated carbon dioxide partial pressure. *Tree Physiology*, **21**, 915–923.
- Valentini R, Matteucci G, Dolman AJ *et al.* (2001) Respiration as the main determinant of carbon balance in European Forests. *Nature*, **404**, 861–865.
- Wang Y-P, Leuning R (1998) A two-leaf model for canopy conductance, photosynthesis and partitioning of available energy I: model description and comparison with a multi-layered model. *Agricultural and Forest Meteorology*, **91**, 89–111.
- Wilson KB, Baldocchi DD, Hanson PJ (2000) Spatial and seasonal variability of photosynthetic parameters and their relationship to leaf nitrogen in a deciduous forest. *Tree Physiology*, **20**, 565–578.
- Wofsy SC, Goulden ML, Munger JW *et al.* (1993) Net exchange of CO₂ in a mid-latitude forest. *Science*, **260**, 409–425.
- Wullschlegel SD, Norby RJ, Love JC, Runck C (1997) Energetic costs of tissue construction in yellow-poplar and white oak trees exposed to long-term CO₂ enrichment. *Annals of Botany*, **80**, 289–297.
- Zak DR, Pregitzer KS, King JS, Holmes WE (2000) Elevated atmospheric CO₂, fine roots and the response of soil microorganisms: a review and a hypothesis. *New Phytologist*, **147**, 201–222.

Appendix: Estimating the vertical profile of PPFD

Leaf area density dynamics

The vertical profile of leaf area index (L in $\text{m}^2 \text{m}^{-2}$) and its seasonal variation for *P. taeda* were obtained by measuring plant area index (Lai *et al.* 2000, LiCor, Lincoln, NE, USA) during winter when the broadleaf species were leafless and *P. taeda* was at minimum L . This profile was expressed on a relative basis, and employed with L obtained based on allometric relationships and L dynamics to estimate the dynamics of the profile (Kinerson *et al.*, 1974; Pataki *et al.*, 1998; Schäfer *et al.*, 2002). L of broadleaf species was estimated as in Schäfer *et al.* (in review) and distributed vertically based on allometric relationships derived from individuals at this site. Seasonal L dynamics of deciduous broadleaf species was assumed to correspond to the time series of the increase in the maximum sap-flux density, obtained from boundary line analysis on data

collected between the time in which bud break was observed and the time of full leaf expansion; a similar dynamics was employed between the onset of chlorosis and full senescence (Oren & Pataki, 2001).

The vertical distribution of current- and previous-year foliage was accounted for by 'growing' the canopy in relation to needle elongation measured for 5 years without a noticeable CO₂ effect (Rogers & Ellsworth, 2002). The observations made at three vertical positions in the canopy demonstrated that needle elongation, expressed cumulatively for all flushes, was nearly linear with time since bud break until full expansion, but was completed 20 days earlier at the bottom of the canopy than at the middle, and 40 days earlier than at the top. Thus, from bud break until day-of-year 210 in which needle elongation at the bottom of the canopy was complete, the increase in leaf area was partitioned vertically in proportion to the leaf area density profile observed at bud break. Thereafter, during the following 40 days before needle elongation ceased at the top of the canopy, leaf area increases were restricted to progressively higher levels in the canopy, removing 1/40th of the total canopy length per day before distributing the daily increase in leaf area in proportion to the leaf area density profile of the remaining actively growing canopy. The decrease in *P. taeda* leaf area index with senescence at the end of the growing season was partitioned vertically in proportion to the amount of previous-year foliage.

Partitioning of incoming radiation

Incoming *PPFD* was partitioned into direct and diffuse components according to Erbs *et al.* (1982):

$$K_T = \frac{I_o}{I_{ex}} \quad (A1)$$

where K_T is the clearness index, I_o is total incoming radiation and I_{ex} is total extraterrestrial radiation. K_T is related to the fraction of the diffuse component by the following:

$$\begin{aligned} \text{if } K_T \leq 0.22 \text{ then } I_d/I_o &= 1.0 - 0.09 \times K_T \\ \text{if } 0.22 < K_T < 0.80 \text{ then } I_d/I_o &= 0.95 - 0.16 \times K_T \\ &+ 4.38 \times K_T^2 - 16.63 \times K_T^3 + 12.33 \times K_T^4 \\ \text{if } K_T \geq 0.80 \text{ then } I_d/I_o &= 0.16. \end{aligned} \quad (A2)$$

where I_d is diffuse radiation.

Vertical distribution of *PPFD*

Direct beam radiation

The extinction coefficient for the direct beam radiation K_{be} is calculated according to Campbell & Norman (1998) as

$$K_{be}(\kappa) = \frac{\sqrt{x^2 + \tan^2 \kappa}}{x + 1.744(x + 1.182)^{-0.733}} \quad (A3)$$

where K_{be} is the light extinction coefficient for ellipsoidal distributed leaves in the canopy, κ is zenith angle (which depends on time of year and time of day), and x is the ratio of average projected leaf area of canopy elements on the horizontal and vertical surfaces (e.g. for a spherical leaf distribution $x = 1$, chosen for this canopy composed mostly of conifers based on Campbell & Norman, 1998). From K_{be} the transmission coefficient (τ_b) is computed, which determines light attenuation of the direct beam through the canopy:

$$\tau_b(\kappa) = e^{(-K_{be}(\kappa) \times L_{ti} \times \Pi)} \quad (A4)$$

where L_{ti} is cumulative leaf area density in layer i , Π is the clumping factor (Campbell & Norman, 1998; Stenberg, 1998). The coefficients for the broadleaf species were assumed to be similar to the values of the more prevailing, canopy dominant *P. taeda* (see Table 2, Schäfer *et al.*, 2002). The direct beam radiation enjoyed by the leaf in each layer (I_{bi}) can be computed as follows:

$$\text{for } P. \text{ taeda, } I_{bi} = K_{be} \times I_b \times c^k \quad (A5a)$$

$$\text{for broadleaf, } I_{bi} = K_{be} \times I_b. \quad (A5b)$$

where I_b is the direct beam radiation above the canopy, c is a coniferous shoot specific transmission coefficient and k is the number of shoots obstructing the light beam in each light category ($k = 0, 1, 2, \dots, 9$).

Diffuse radiation

The light extinction coefficient for diffuse radiation (K_d) is a function of L_{ti} and thus changes throughout the canopy. After obtaining K_d from the K_d - L_{ti} relationship shown in Campbell & Norman (1998), the transmission coefficient for diffuse light (τ_d) is computed as

$$\tau_d = e^{(-\sqrt{x_p} \times K_d(L_{ti}) \times L_{ti})} \quad (A6)$$

where parameters are as in Eqn (A4) and where x_p is leaf absorptivity of *PPFD* (see Table 2). The diffuse radiation in the i th canopy layer (I_{di}) is computed as for *P. taeda* and the broadleaf canopy by:

$$I_{di} = I_d \times \tau_d, \quad (A7)$$

where I_d is diffuse radiation above the canopy (see also Eqn (A2)).

Scattered radiation

Scattered radiation is created by reflection of radiation from the leaves. The transmission coefficient for scattered radiation (τ_s) is computed by using the

extinction coefficient of the direct beam K_{be} (Eqn (A3)),

$$\tau_s(\kappa) = e^{1 - \sqrt{2} \times K_{be}(\kappa) \times L_{ti} \times \Pi}, \quad (\text{A8})$$

and the scattered radiation in the i th canopy layer (I_{sc}) can be computed as

$$I_{sc} = (\tau_s - \tau_b) \times I_b. \quad (\text{A9})$$

The three radiation types were combined at each canopy level to calculate the light intensity incident on the leaf surface in each of the 10 light categories.

Proportion of foliage in each PPFD category

For estimating stomatal conductance and C_i/C_a broadleaf foliage was assigned to two categories (sunlit vs. shaded) and *P. taeda* foliage was assigned to 10 categories of varying PPFD ranges. For broadleaf species, the amount of sunlit and shaded foliage was estimated throughout the canopy as the fraction that receives sunlight at each canopy depth, according to Campbell & Norman (1998):

$$f_{sl}(\kappa) = e^{(-K_{be}(\kappa) \times L_{ti})} \quad (\text{A10a})$$

where f_{sl} is the fraction of sunlit leaves at depth i as a function of the zenith angle κ which depends on time of year and time of day (Campbell & Norman, 1998). Shaded foliage was illuminated with diffuse and scattered light, while sunlit foliage enjoyed direct light in addition. For *P. taeda*, a penumbral effect resulting from coniferous shoot structure distributes direct light into intensity regimes below that of the unobstructed light (Stenberg, 1998); thus, the probability of light

category f_{sl} in the i th canopy layer is

$$f_{sl}(k) = \frac{(K_{be} \times L_{ti} \times \Pi)^k}{k!(1-c)^k} \times e^{\left[\frac{K_{be} \times L_{ti} \times \Pi}{1-c} \right]}. \quad (\text{A10b})$$

Canopy conductance was distributed vertically separately in the broadleaf and *P. taeda* canopy. In the broadleaf canopy the fraction of conductance of each foliage category in each layer relative to the total was used as weights to rescale the mean canopy stomatal conductance (G_C) obtained from sap-flux, such that the total water uptake would be preserved, as

$$\begin{aligned} G_C &= G_S \times L \\ &= \sum_{i=1}^n (g_{sli} \times L_i \times f_{sli} + g_{shl} \times L_i \times (1 - f_{sli})), \end{aligned} \quad (\text{A11})$$

where G_S is mean stomatal conductance for hardwoods, L is leaf area index, i is canopy layer, n is number of canopy layers (here $n = 16$), g_{sl} and g_{sh} is stomatal conductance of sunlit and shaded foliage, respectively, and f_{sl} is sunlit fraction of the foliage. In the *P. taeda* canopy a penumbral effect on the PPFD distribution within the canopy of *P. taeda* was incorporated according to Stenberg (1998). Accounting for this effect, the foliage in each canopy layer was divided into 10 light categories. Using a similar weighting methodology to that described above for the broadleaf canopy, G_C of *P. taeda* was repartitioned such that

$$G_S \times L = \sum_{i=1}^n (g_{ij} \times L_{ij} \times k_j), \quad (\text{A12})$$

where j represents the light class, and k_j is the probability of light category j (Stenberg 1998).